THE THERMAL-MECHANICAL BEHAVIOR OF A MULTIPLE-LOOP GEOTHERMAL HEAT EXCHANGER PILE

By
ROMAN POUDYAL

Bachelor of Science in Civil Engineering
Tribhuvan University
Kathmandu, Nepal
2010

Submitted to the Faculty of the
Graduate College of the
Oklahoma State University
in partial fulfillment of
the requirements for
the Degree of
MASTER OF SCIENCE
December, 2014

THE THERMAL-MECHANICAL BEHAVIOR OF A

MULTIPLE-LOOP GEOTHERMAL HEAT

EXCHANGER PILE

Thesis Approved:

Dr. Xiaoming Yang

Thesis Adviser

Dr. Rifat Bulut

Dr. Julie Ann Hartell

ACKNOWLEDGEMENTS

First of all, I would like to thank my friends and family here and back home for their love and support during my graduate studies.

I would like to express my deepest gratitude to my advisor, Dr. Xiaoming Yang, for his continuous assistance and guidance throughout my research. You are mentor and you have always inspired me by your leadership, enthusiasm, and welcoming nature. Special thanks to Dr. Rifat Bulut and Dr. Julie Ann Hartell for serving on my thesis committee and providing valuable suggestions for improvement. I also like to thanks Dr. Jeffrey D. Spitler for his guidance during the research.

I am deeply thankful to Matt Mitchell for his great help in building heat exchanger pipes, setting up test trailer and running the test. Without your help I could not have made it possible. And I would like to express my thanks to: Kristi Bumpass (Red Rock Consulting, LLC) for conducting soil exploration drilling, Spencer Enterprises Inc. for installing the test pile, IGSHPA for providing the experimental site, and my colleagues Omar Moudabel and Spandana Annamraju for their help in lab and field works.

And finally to many others who contributed to this work.

Name: ROMAN POUDYAL

Date of Degree: DECEMBER, 2014

Title of Study: THE THERMAL-MECHANICAL BEHAVIOR OF A MULTIPLE-LOOP GEOTHERMAL HEAT EXCHANGER PILE

Major Field: CIVIL ENGINEERING

Abstract:

Geothermal heat exchanger pile (GHX-pile) is an innovative technique of utilizing heat energy stored in the Earth. However, the technique lacks standard design guidelines considering the behavior of the pile with thermal and mechanical load. Most of the studies done till date focus on the heat exchange behavior of small size piles with only single or double loops. There is a lack of knowledge on the geotechnical aspect of GHX-piles system with multiple loop large-diameter bored piles which are more common in larger structures. Therefore, the current study focuses on the investigating thermal-mechanical behavior of a full-scale GHX-pile. The GHX-pile was thermally loaded by conducting a thermal response test. A modified t-z model was developed and applied to simulate the test result. Parametric analysis was performed with the modified t-z model and combined effect of thermal and mechanical loads on the GHX-pile was investigated. The research results indicated that the heating load increases the axial force mobilization in the GHX-pile. However, in case of loaded pile the change in the mechanical response of the GHX-pile due to thermal load is small. Parametric study showed that the heating load helps to reduce the top displacement, while the cooling load increases the top displacement.

TABLE OF CONTENTS

LIST OF TABLES

LIST OF FIGURES

CHAPTER 1

INTRODUCTION

1.1 BACKGROUND

Global warming has become a major concern of the modern society. The current rate of the global warming must be controlled for maintaining the balance of the ecosystem. One of the major causes of global warming is the emission of carbon-dioxide (CO_2) from the burning of fossil fuels for electricity and heat. Therefore, the development and use of renewable energies with lower CO_2 emission or with lower impact on the environment is necessary. Geothermal energy is one of the renewable energy sources. Heat presented underneath the ground surface may be used as an energy source. The geothermal energy may be extracted from different depths inside the crust of the Earth. Deep geothermal energy is from the hot water/rock in the deeper portion of Earth's crust whereas shallow geothermal energy is from heat presented in the shallow depths of Earth's surface.

Shallow depth geothermal energy has been used for the heating and cooling operations of buildings with the help of a heat pump. This system is generally known as the ground source heat pump (GSHP) system. Some studies showed that GHSP system can reduce the emission of greenhouse gas by 66% or more compared to traditional methods of heating and cooling (Mustafa Omer 2008).

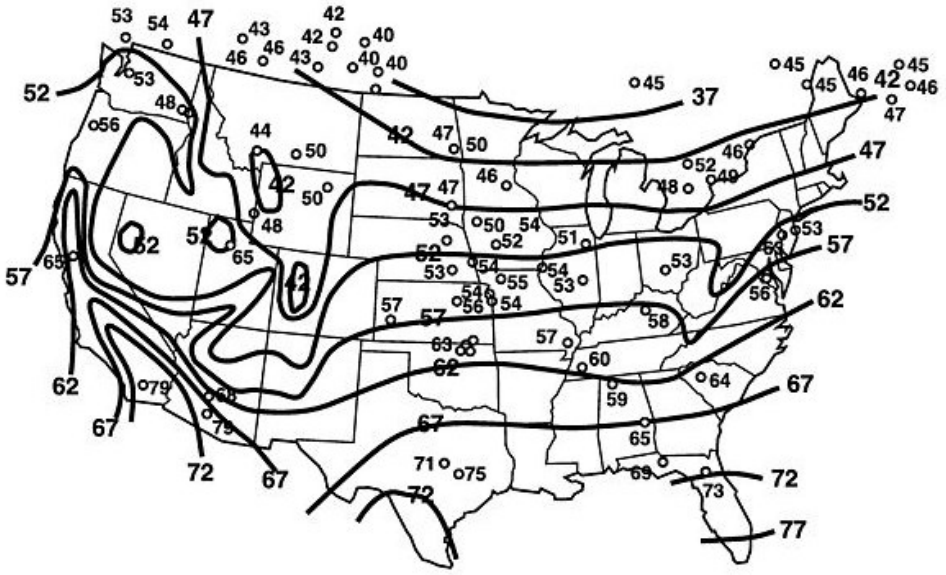

Figure 1-1: Contour of mean annual ground temperature in different parts of the United States (BuilditSolar, 2014)

Ground temperature remains nearly constant below a certain depth. Generally at 5 m depth of the earth surface the ground temperature is around 10-18° C (50-65° F) depending on the location (Kusuda and Achenbach 1965). The mean ground temperatures in different parts of the United States are shown in Figure 1-1. The upper surface of ground exhibits a temperature variation with respect to surrounding temperature, but the temperature below that remains almost constant. This property of earth is utilized in the GSHP system as a constant temperature source/sink in heating/cooling operations. In the heating cycle (during winter), the temperature of earth is higher than the surrounding atmospheric temperature, so it is used for extracting the heat and treated as a heat source. In the cooling cycle (during summer), the earth temperature will be lower than the surrounding atmospheric temperature, so it is used for rejecting the heat and treated as a heat sink. Heat is exchanged between the ground and the heat pump system through heat exchanger polythene pipes generally filled with water.

A GSHP system generally consists of heat exchanger pipes, heat pump, and the heat distribution system. Heat exchangers are high density polythene pipes consisting of water (sometimes mixed with antifreeze) as heat transfer fluid, and they are mainly horizontal and vertical types. The schematic diagram of a GSHP system consisting of horizontal and vertical heat exchangers (loops) is shown in Figure 1-2. Both horizontal and vertical heat exchangers are connected to the heat pump system which exchanges heat between the Earth and the building. Shallow trenches have to be excavated for laying horizontal loops, whereas small drill holes have to be constructed for vertical loops. Large open surface area is needed for installation of horizontal loops, so vertical loops are more suitable when available installation area is limited. The shallow trenches shows temperature variations with respect to solar radiation, wind, and rain, whereas temperature in the vertical drill holes remains almost constant throughout the year. Also, in vertical drill holes heat transfer rate is increased by flow of ground water table. Thus, the vertical loops are more efficient than the horizontal loops. A GSHP system only requires energy input for running the heat pump, and its maintenance and running cost is low. A GSHP system utilizes electrical energy to convert heat energy from the ground at 10-15° C to a temperature of 25-35°C which is required for heating and cooling operations (Brandl 2006). Also it has more coefficient of performance (heat output for a unit input of electrical energy) than traditional air source heat pump systems (Hwang et al. 2010). But the need for extra space for the installation of heat exchangers and the cost of installation makes the GSHP more expensive than the installation of the traditional air conditioning system.

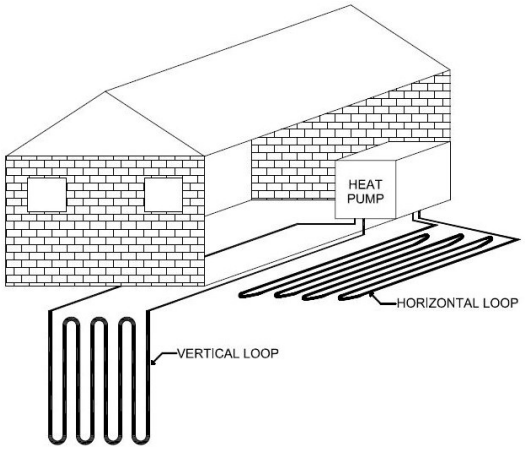

Figure 1-2: Ground source heat pump system (GSHP) with horizontal and vertical heat exchangers loops

In order to offset the installation cost of a GSHP system, an innovative technique is to build geothermal heat exchanger piles (GHX-pile), in which building foundations (mainly piles) and heat exchanger pipes are combined (Péron et al. 2011). Since there is no need for additional drilling, the installation cost of the GHX-pile is less than the installation of the GSHP system. Figure 1-3 shows the schematic diagram of a GHX-pile system. It consists of three main parts: an earth connection via heat exchanger enclosed in the pile foundation, pump system, and heat distribution system (Mustafa Omer 2008). As stated earlier, in the summer (cooling phase), the atmospheric temperature is higher than the ground temperature, so the heat exchange fluid releases heat to the ground. This process causes a reduction in fluid temperature in the pipes while coming out from the pile foundation ($T_{out} < T_{in}$). This condition just reverses in winter (heating phase) ($T_{out} > T_{in}$). In Figure 1-3 the red color symbolizes the flow with higher temperature and the blue color symbolizes the flow with lower temperature. Figure 1-4 shows a close view of a GHX-pile constructed with a U-shaped 8 pair of heat exchanger pipes. Brandl (2006) have listed many benefits of the GHX-pile system such as a sustainable and renewable

energy source, lower running costs and longer life, higher safety and durability because of closed loop enclosed in the structure, and less space requirement.

Though GSHP with GHX-pile seems to be a promising technology, it lacks standard design guidelines for describing the interaction and behavior of soil and added structural component on application of the thermal and mechanical load (Péron et al. 2011). Much research has been done in the field of GSHP, but most of it has been in borehole heat exchanger systems. The GHX-pile being relatively new technology still needs studies and experiments to investigate the behavior of pile and to know its heat extraction/injection capacity. Furthermore, most of the previous test studies used relatively small diameter piles (less than 600mm in diameter) with only one or two vertical loops inside. There are only a limited number of researches on larger diameter piles which are more common in high-rise buildings and structures. To incorporate GHX-pile system in high-rise buildings structures, it is necessary to quantify how much heat can be extracted/injected from each pile and how many heat exchanger loops are needed for optimum performance. The structural impact (stress/strain development) on the pile and the pile-soil interaction should also be quantified.

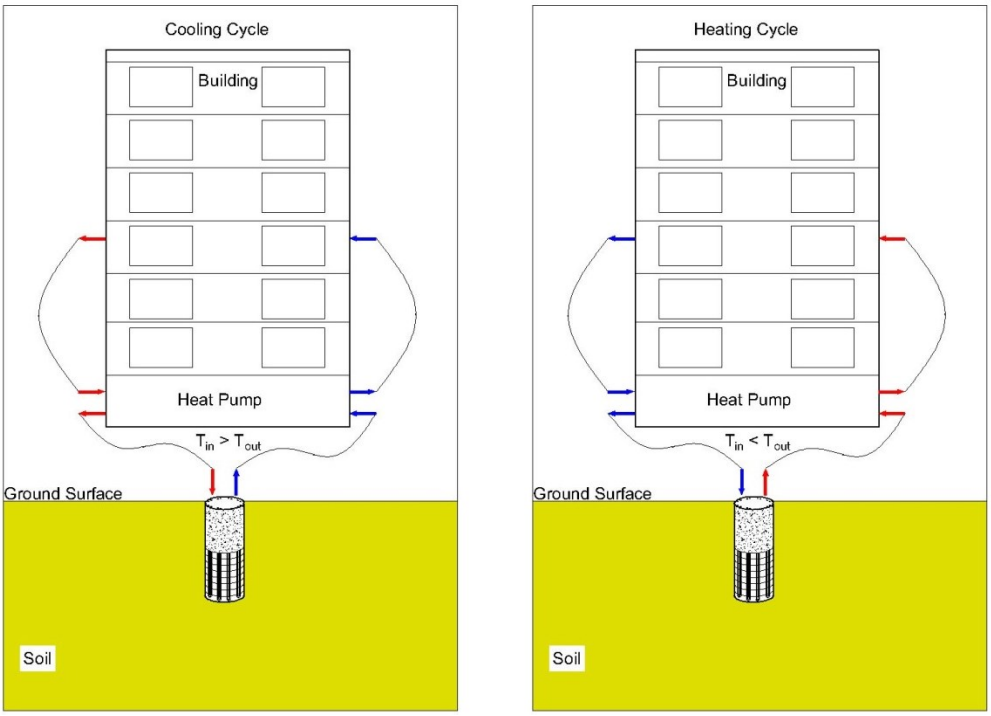

Figure 1-3: Ground source heat pump system with GHX-pile

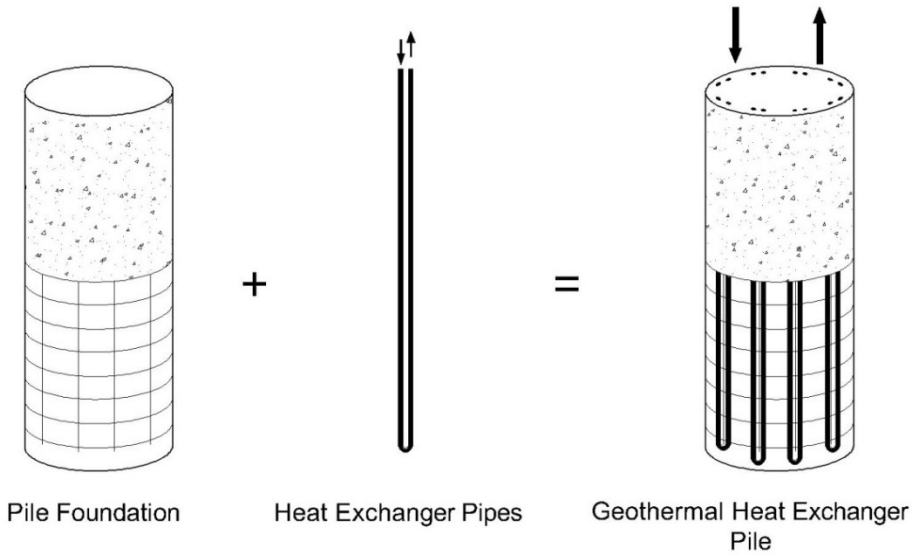

Figure 1-4: Geothermal heat exchanger pile (GHX-pile)

1.2 SCOPE OF STUDY

The current study was focused on investigating thermal-mechanical behavior of a full-scale GHX-pile. A 1.067-m diameter bored pile (also called drilled shaft) was constructed on the campus of Oklahoma State University (OSU). Thermal loading was applied by running a thermal response test on the test pile. In the thermal response test, a constant rate of heat was supplied to the pile by circulating heat exchanger fluid in the heat exchanger pipes. The strain development in the pile, the temperature change of the pile, the flow rate of heat exchanger fluid, and the heat exchanger fluid temperature were recorded during testing.

In order to investigate the thermal-mechanical behavior of the pile, a modified t-z model was applied to simulate the test result. After the calibration of soil/rock properties against the test data, a parametric analysis was performed with the modified t-z model. Although only a thermal load was applied in the field test, the combined effect of thermal and mechanical loads was investigated in the parametric analysis.

1.3 OBJECTIVE OF STUDY

The objectives of the study are:

- to check the applicability of line source model in analyzing thermal response test data of larger-diameter GHX-pile;
- to observe changes in stress/strain in the GHX-pile under thermal loading;
- to develop a load displacement (t-z) model using the load transfer concept; and

- to investigate thermo-mechanical behavior of the GHX-pile using a parametric analysis.

1.4 ORGANIZATION OF THESIS

This thesis consists of six chapters. Following this chapter, Chapter 2 reviews some theoretical concepts, parameter, and tests which are necessary in understanding and analyzing the GHX-pile system. Chapter 2 also reviews major research and development done in this field based on published literatures. Chapter 3 describes the test pile construction, experimental setup, and the test procedure. Chapter 4 presents data obtained from the field test. Chapter 5 presents analysis and discussion of results. This chapter also includes development of a modified t-z model and the parametric analysis results. Finally, Chapter 6 presents conclusions of the current work and recommendations for future research.

CHAPTER 2

LITERATURE REVIEW

2.1 THERMAL PROPERTIES OF SOIL

Thermal properties of the soil are important governing factors in the GHX-pile design. Heat extraction/injection is done in heating and cooling process utilizing the ground as a source and a sink. The design of the GHX-pile and the number of the heat exchangers required depend on the thermal properties of the ground (soil). The most important soil thermal properties are: thermal conductivity (k), specific heat capacity(c), and thermal diffusivity (α). These properties depend on the soil's types, composition, water content, density, and soil constituents (mineralogical content).

Thermal Conductivity of Soil (k)

Heat passing in unit temperature gradient in the direction of heat flow through a unit cross sectional area in a unit period of time is defined as the thermal conductivity of the soil. It is measured in Watt per meter per Kelvin (W/mk) or also in British thermal unit per foot hour per Fahrenheit (Btu/ft.hr.°F). There are various methods for measuring or estimating this parameter including empirical formulas, laboratory tests, and in-situ tests.

Many empirical formulas based on the soil properties (water content, saturation, porosity) are available for the estimation of k with the accuracy of ±25% (Farouki 1986). The range of k values for the different group of soil/rock types are available in 'Soil and Rock Classification for the Design of Ground-Coupled Heat Pump Systems: Field Manual' (Salomone et al. 1989).

Steady state and transient state are two basic principles used in both laboratory and in-situ tests. Guarded hot plate tests (ASTM C1044 and ASTM C177), cylindrical apparatus test (Kersten 1949), and needle probe method (ASTM D5334) are some standardized laboratory tests for measuring the soil thermal conductivity. The first two tests are based on the steady state principal while third test is based on the transient state principle. Needle probe method is also used in the in-situ tests.

In-situ tests of the thermal conductivity of soil are based on the borehole test method. Constructing the borehole and utilizing it for determination of soil thermal conductivity is a must accurate method (Bose et al. 2002). Development of a trailer equipped with the different systems required for determining soil thermal properties (conductivity) is described in (Austin 1998). Same trailer had been used in this research for applying the thermal load to the pile. Typical soil thermal conductivity values are presented in Table 2-1.

Table 2-1: Soil Thermal Properties Soil (Salomone et al. 1989)

Thermal Texture Class	Thermal Conductivity		Thermal Diffusivity	
	W/m°K	Btu/ft hr °F	cm^2/sec	Ft^2/day
Sand (or gravel)	0.77	0.44	0.0045	0.42
Silt	1.67	0.96	-	-
Clay	1.11	0.64	0.0054	0.50
Loam	0.91	0.52	0.0049	0.46
Saturated Sand	2.50	1.44	0.0093	0.86
Saturated Silt or clay	1.67	0.96	0.0066	0.61

Specific Heat Capacity (c)

Specific heat capacity is the amount of energy needed to change the unit temperature of the unit soil mass. It is measured in J/kgK and can be determined by adding the heat capacities of different constituents of the soil as per volume. Thermal capacity of the soil increases with an increase in water content but decreases in case of freezing (ice has less heat capacity than water) (Brandl 2006). Brandl (2006) further explains the simple procedure for determining heat capacity in laboratory by mixing soil and water at different temperatures. The prepared mixture was allowed to reach thermal equilibrium within the system without heat loss to the surroundings. Then the specific heat capacity of soil is determined from the known specific heat capacity of the water. Generally dry soil at 0°C and water at 20°C are mixed. If moist soil is used, correction should be applied for moisture content.

Thermal Diffusivity (α)

Thermal diffusivity is the property which determines how easily and rapidly soil can change the temperature. It is derived from the other two parameters of soil: thermal conductivity (k) and specific heat capacity (c). Thermal diffusivity is expressed in square meter per second (m^2/s).

$$\alpha = \frac{k}{\rho * c}$$

where, ρ = density (kg/m^3).

2.2 HEAT TRANSFER IN SOIL

Conduction, convection, and radiation are main mechanisms that account for the heat transfer in the soil. Conduction is the dominant way of heat flowing in soil while convection and radiation are less dominant. Convection also becomes dominant if high flow rate of groundwater is present in the soil (Rees et al. 2000). If both pore size and particle size of the soil are small in comparison to the total volume of the soil than heat transfer in the soil can be considered by conduction only.

2.3 HEAT TRANSFER IN CONCRETE

Heat transfer in the concrete is governed by three thermal properties: thermal conductivity (k_c), specific heat capacity (c_c) and thermal diffusivity (α_c). Concrete has good thermal conductivity and thermal storage capacity, which makes it a perfect material to enclose the heat exchanger pipes. Thermal conductivity depends on aggregate contents and types of aggregate and presence of moisture in the concrete (Marshall 1972). Conductivity of concrete varies from 1 to 1.5 W/mK. When specific details information about the aggregate proportion in the pile concrete and their properties, types are not known; the pile thermal conductivity should not be assumed more than 1.5 W/mK (GSHPA, 2012).

It is good to use concrete with higher thermal conductivity. More aggregate with higher conductivity should be used in concrete mix. But the concrete mix design mainly determined by structural design as primary function of the pile is to provide structural support.

2.4 HEAT TRANSFER AND PIPE FLOW

Heat transfer occurs between fluid and surface when there is a temperature difference between the fluid and the surface. This transfer process is called convection (or advection). This phenomenon governs the heat transfer from heat exchanger fluid to the pipe wall and the heat transfer rate is expressed as;

$$\frac{Q}{A} = h(T - T_f)$$

where, Q/A = rate of heat transfer, h = heat transfer coefficient (watt/m^2k), T = temperature of surface and T_f = fluid temperature.

Rate of heat transfer between fluid and surrounding pipe depends on the type of flow in the pipe (laminar or turbulent flow). Velocity and pressure at different point in the turbulent flow regime fluctuates with time which creates better heat transfer nature than the laminar flow. Hence it is better to achieve the turbulent flow in the heat exchanger pipes. Laminar and turbulent flow is determined based on the Reynolds number (R_e). If R_e is less than 2300, the flow is designated as a laminar flow and if it is more than 4000 as a turbulent flow.

$$R_e = \frac{\rho * u_m * d}{\mu}$$

where, u_m = mean velocity (m/sec), d = diameter of pipe(m), ρ = fluid density (m^3/sec) and μ = fluid viscosity ($N \cdot s/m^2$).

The amount of heat injected or absorbed can be estimated based on the pipe inlet and outlet flow temperature using following equation;

$$Q = mc(T_{Out} - T_{in})$$

where, m = mass flow rate of fluid in the pipe (kg/s), c = specific heat capacity of the fluid (J/kg K), T_{in} = temperature of the fluid entering the pipe , T_{out} = temperature of the fluid leaving the pipe.

2.5 RESEARCH AND DEVELOPMENT of GHX-PILE

Geothermal energy has been used for a long time directly or by-producing electricity. First production of commercial geothermal electricity was done in 1913 (Fridleifsson and Freeston 1994). Utilization of the geothermal energy has increased rapidly in different forms, ground source heat pump, bathing and swimming, space heating, green house and open space heaters, aquaculture, and raceway heating (Lund et al. 2011). GSHP space heating and cooling requires the heat exchanger buried in the ground. Installation of the horizontal and the vertical heat exchanger requires additional space and increase cost in building construction. So, utilization of the foundation piles for installing the heat exchanger reduce additional cost and brings new innovative way in the GSHP system (Abdelaziz et al. 2011).

Use of foundations for extracting the geothermal energy had begun from 1980s in Austria and Switzerland. First base slab of a building then in 1984 the pile foundation of the building was used to use geothermal energy (Brandl 2006). Being new technology, it is still undergoing more research and testing for developing the design standards and guidelines. A number of researches have brought light to the use of the GHX-piles, but still most of the studies focus on the heat exchange behavior of the small size piles. There is a lack of knowledge on the geotechnical aspect of GHX-piles system with large-diameter bored piles which are more common in the large structures. Based on the review of the research and development in this field, it is found that most studies have been done in piles with smaller diameters ranging from 200 mm to 600 mm. There are some studies available on larger GHX-piles (Jung et al. 2013; Ooka et al. 2007) but not all of the information from these tests has been published; so there is a need for field tests and analysis of larger GHX-piles. Péron et al. (2011) explain that due to the lack of understanding of pile structure behavior and soil behavior on the application of thermal and mechanical loading, and also due to lack of standard design guidelines, a large factor of safety is used in designing GHX-piles. Singh et al. (2011) listed different questions that needed to be investigated about GHX-pile, for example, the effect of heat on the pile and its capacity, the amount of heat transfer and storage in soil and pile, the effect on soil due to heat, and reasons to move from old system to the new system of heating and cooling based on its cost and feasibility. Here, major field study and GHX-pile operational systems available in published literature had been summarized in Table 2-2.

Table 2-2: Field test and operational system

Location	Pile			Heat Exchanger		Test Description			Reference
	Type	Diameter (mm)	Depth (m)	Type	Loop Number per pile	Type	Loading (kN)	Input temperature (°C)	
Geneva, New York, USA	Steel tube with concrete	200	26	U	1	Thermal	-	4 to 27	(Henderson et al. 1998)
Bad Schallerbach Austria	Pile raft	1200	9	U	-	Thermal and Mechanical	Max 900	-	(Brandl 1998)
Frankfurt, Germany	-	1500	20 to 30	-	-	Thermal	-	-	(Quick et al. 2005)
Lausanne, Switzerland	Pile raft	880 (average)	25.8	U	2	Thermal and Mechanical	Max 1300	21	(Laloui et al. 2006)
Zuric Airport, Switzerland	Bored	900 to 1500	26.8	U	5	Thermal	-	Min 2.4	(Pahud and Hubbuch 2007)
Sapporo, Japan	Hollow precast concrete	302	9	U	1,2	Thermal	-	17.8,18.9	(Hamada et al. 2007)
Chiba, Japan	Cast in-place	1500	20	U	8	Thermal	-	-	(Ooka et al. 2007)
Shanghai, China	Bored	600	25	U W	1,2,3 1	Thermal	-	32,35,38	(Gao et al. 2008)
Lambeth college, United Kingdom	Friction pile	600	23	U	2	Thermal and Mechanical	Max 1800	-6 to +56	(Bourne-Webb et al. 2009)
Nottingham, United Kingdom	Deep continuous flight auger	300	10	U	1	Thermal	-	35	(Wood et al. 2010)
Richmond, Texas	Auger pressure grouted	300 and 450	18.3	U	2	Thermal	-	40-45	(Brettmann and Amis 2011)
Clayton Campus, Australia	Bored	600	18	U	3	Thermal and Mechanical	Max 1885	-	(Singh et al. 2011)
Pusan, South Korea	Cast in-place	1500	60	W S	-	Thermal	-	-	(Jung et al. 2013)

2.6 THERMAL RESPONSE TEST

Thermal response test (TRT) is a technique for evaluating the ground thermal conductivity, thermal resistance of pile, and the general performance of the ground and the heat exchangers. The test is done by injecting heat to the ground via heat exchanger fluid at constant rate. Corresponding inlet and outlet temperature of the fluid during test is measured. This technique was originally developed by Mogensen (1983) for the borehole heat exchangers.

For the first time in 1996 independently both in Sweden and USA, mobile TRT device was developed which was then followed by development of similar test devices in other countries (Gehlin 2002). In Oklahoma State University, a trailer with all necessary equipment was developed. Detail description of this instrument was provided by Austin (1998) and the same instrument was used in current research for applying thermal load to the pile.

TRT was developed for the borehole heat exchanger, so well established guidelines are available for conducting the experiment and analysing the obtained data from the test. Data collected from TRT are analysed using different analytical, numerical and mathematical models. The line source model is the most common model used to analyse the data. Line source model is developed by Kelvin (Ingersoll et al. 1948). This theory was used by Ingersoll and Plass (1948) in the borehole heat exchangers and later Mogensen (1983) used this theory to find out the thermal conductivity of the soil. In this theory, heat exchanger is replaced by the needle shaped heat source neglecting its radial

dimension. Heat exchanger is assumed as an infinite line source with constant heat flux in the ground. Ground is supposed as an infinite medium. Heat flow pattern is simplified only in lateral direction. Axial flow, flow above the top across the ground and below the bottom of the heat exchanger is neglected (Yang et al. 2010). The general line source equation (Carslaw and Jaeger 1959) is shown below:

$$T(r,t) - T_0 = \frac{q}{4\pi k}\int_{\frac{r^2}{4\alpha t}}^{\infty} \frac{e^{-u}}{u} du = \frac{q}{4\pi k} E_1(r^2/4\alpha t)$$

where, t= time, r = radial distance, T= temperature of the flow, T_0 = initial temperature of the ground, q = heating rate per length, k = thermal conductivity, α = thermal diffusivity, and E_1 = exponential integral.

For large value of $\alpha t/r^2$ exponential integral can be expressed as follows;

$$E_1(r^2/4\alpha t) = ln\left(\frac{4\alpha t}{r^2}\right) - \gamma$$

where, γ is Euler's constant (0.57721)

Fluid temperature (T_f) in TRT is evaluated considering the thermal resistance of borehole (R_b) and the ground temperature increase. Considering these factors, the above equation is converted to:

$$T_f = \frac{q}{4\pi k}\left\{ln\left(\frac{4\alpha t}{r^2}\right) - \gamma\right\} + qR_b + T_0$$

For evaluation of the thermal conductivity of the borehole, Mogensen (1983) converted above equation to the following form based on steady state condition;

$$\Delta T(r,t) = \frac{q}{4\pi k}\left\{ln\left(\frac{4\alpha t}{r^2}\right) - \gamma\right\} + qR_b + \frac{q}{4\pi k}\ln t$$

In above equation, the first two terms on the right hand side are constant, so the equation is similar to linear slope equation (Y = mX + C). The slope from the steady state portion of temperature vs ln(t) graph then can be used to calculate the thermal conductivity of the ground.

$$Slope = \frac{q}{4\pi k}$$

$$K = \frac{q}{4\pi * Slope}$$

Thermal Response Test in Pile Foundation

There is less information and guidelines available for using TRT in the pile foundations. GSHPA (2012) had published guidelines regarding the design, installation of geothermal piles, and included guidelines for conducting the TRT test in the geothermal piles. Following are four main points in the guidelines;

- If in any geothermal heating cooling system need of GHX-pile is warranted then it is better to construct the borehole to test thermal properties of soil by running the TRT test.
- If the pile size is less than or equal to 300 mm, TRT can be done following same guideline of the boreholes.
- If the pile size is more than 300 mm, TRT test should be long than the borehole test duration and data obtained need more sophisticated analysis.
- It is better to monitor temperature induced stress and strain during the test to evaluate structural impact of the thermal load.

Test duration of TRT for the pile should be longer enough so that the resistance of the pile should be overcome and response shown should be of the ground on test results. On using the line source method analysis data up to time t_{min} from beginning of the test is discarded to neglect the effect of the borehole or pile resistance on data obtained. t_{min} calculated using following relation (Eskilson 1987);

$$t_{min} = \frac{5r^2}{\alpha}$$

where, r = radius of borehole or pile (m) and α = thermal diffusivity of ground (m^2/s)

2.7 LOAD-DISPLACEMENT MODEL

Pile load tests are best way to the know load carrying capacity and the load-settlement behavior of the pile, but these tests are site specific, time consuming, and expensive. So, estimation of movement of axially loaded pile using load transfer approach is a more convenient method. Seed and Reese (1957) first suggested this method by the predicting load transfer curve using data from vane shear test. They have given differential equation representing load transfer mechanism between the pile and the soil in relation with displacement and load transfer functions. Later Coyle and Reese (1966) developed a procedure for predicting the load displacement curve in axially loaded pile using load transfer concept.

In load displacement calculation explained by Coyle and Reese (1966) pile was divided in the small segment connected with each other and soil by spring. Spring connecting the pile segment represents the pile stiffness and connecting to the soil represents pile-soil

interaction. For each divided segment, load and settlement were calculated. Differential equation representing load distribution in axially loaded pile explained by Seed and Reese (1957):

$$\frac{dz}{dx} = \frac{P}{EA}$$

$$\frac{dP}{dx} = EA\frac{d^2z}{dx^2}$$

where, P = axial force in the pile, E = Young's Modulus of Pile, A = cross sectional area of the pile

They further explain the unit friction function (f_s) defining soil load transfer behavior on the side of the pile which when multiplied by the displacement of the pile gives soil shear strength.

$$dP = -f_s * z * dx * \pi * D$$

where, f_s = side load transfer coefficient of soil, D = diameter of the pile, z = displacement of the pile segment, dx = length of the pile segment

Final expression representing the load distribution in an axially loaded pile is as follows:

$$EA\frac{d^2z}{dx^2} = f_s z \pi D$$

Similar explanation of the load displacement calculation using difference form of the above equation is given in Reese et al. (2006).In current study this referenced was followed while developing the load transfer model.

These methods depend on load transfer functions (unit side friction (f_s) and unit end bearing capacity (f_b)) with a corresponding displacement of pile. These functions are obtained from q_s-z (side resistance verses displacement) and q_{end}-z (end resistance verses displacement) curves and varies as per diameter of the pile, stiffness of the pile and soil, soil type, pile length and other soil properties. Frank and Zhao (1982) had suggested using the Menard Pressuremeter Modulus value for estimating load transfer function. These functions will be constant if there is a linear relationship between the pile settlement and the soil resistance (Seed and Reese 1957).

Application of Load Displacement Method in GHX-pile

The load transfer approach to analyze behavior of the geothermal pile was used by Knellwolf et al. (2011). They predicted stress/strain and movement of the pile on application of thermal load based on this theory. They followed the concept developed by Coyle and Reese (1966), and Seed and Reese (1957) and formulated the model to analyze the behavior of the pile on mechanical and thermal loads. They used load transfer functions proposed by Frank and Zhao (1982) based on the Menard pressuremeter modulus value. Thermal load was added to the load displacement model by using null point theory proposed by Bourne-Webb et al. (2009) for the GHX-piles. Null point is no movement point in the pile during thermal loading. Movement of the pile was calculated from the null point along the length of the pile. Validation of this model was done using two field test data EPFL in Lausanne, Switzerland (Laloui et al. 2003, 2006) and Lambeth College in London, United Kingdom (Bourne-Webb et al. 2009).

2.8 PILE BEHAVIOUR ON THERMAL LOADING

Strain developed in the pile in the application of thermal load. Pile tends to expand with an increase in the temperature and tends to contract on decreasing the temperature. So, in the extraction of the heat (heating cycle) pile contract and during injection of the heat (cooling cycle) pile expands. Expansion is noted as negative strain and contraction as positive strain in the current study.

$$\varepsilon_T = \alpha \Delta T$$

where, ε_T = thermal strain, α = coefficient of thermal expansion of concrete (1/°C), ΔT = change in temperature (°C)

If the pile is completely free to deform only thermal strain will be developed no thermal stress. Strain variation in the heating and cooling cycle along the pile surface is seemed as shown in figure based on (Bourne-Webb et al. 2009).

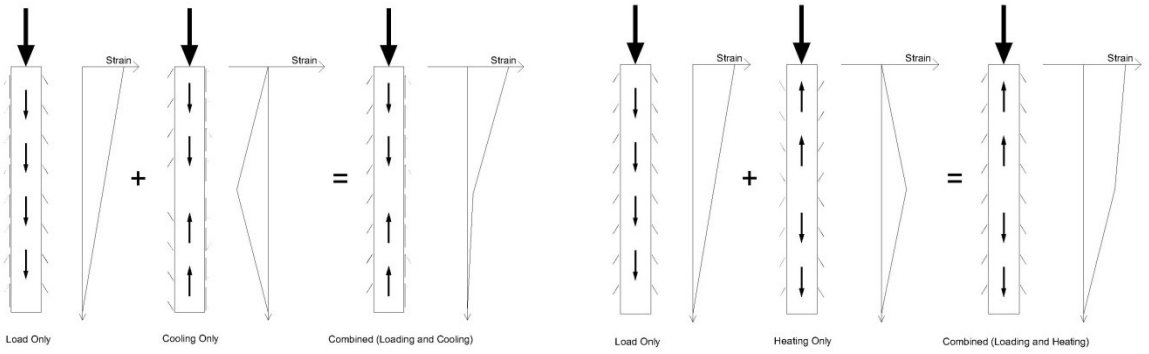

Figure 2-1: Strain variation in heating and cooling cycle along the pile length (reconstructed from Bourne-Webb et al. 2009)

When the expansion or contraction of the pile was restricted by surrounding soil stress was developed. Stress was calculated from blocked strain which is difference of free strain and observed strain. Observed strain is measured strain in the pile during thermal

loading and free strain is the amount of strain that will develop in the pile if the pile is free to expand. So, thermal stress will be:

$$\sigma_T = E(\varepsilon_o - \varepsilon_f) = E * (\varepsilon_o - \alpha \Delta T)$$

where, σ_T = thermal stress (N/m^2), E = Young's modulus of elasticity (N/m^2), ε_o = observed thermal strain, ε_f = free thermal strain

CHAPTER 3

METHODOLOGY

3.1 EXPERIMENTAL SETUP

Geothermal heat exchanger pile of 1.067 m (40 in.) diameter and 12.2 m (40 feet) depth was installed in September 2013. Bored in-situ reinforced GHX-pile was constructed by using auger boring method. After boring, the instrumented reinforcement cage was inserted into the bored hole where concrete mix was poured later. Eight U-loops of 0.0254 m (1 inch) diameter high density polythene (HDPE) heat exchanger pipes were attached to the circumference of the reinforcement cage at equal spacing. A center rod with eight vibrating wire strain gauge were installed. The top strain gauge was installed at 1.1 m (3.5 feet) below top of the pile and the other seven strain gauges were installed at an equal spacing of 1.5 m (5 feet). These sensors were connected to the data logger which was set to record data at an interval of ten minutes. Steps involved in the installation of the GHX-pile are shown in Figure 3-1.

a.

b.

c.

d.

Figure 3-1: Pile installation process. a) Auger boring, b) Installation of pipes and sensor in reinforcement cage, c) Installation of reinforcement cage, d) Concrete Pouring

Heat Exchanger U-loops

Eight U-shaped HDPE heat exchanger loops were made by fusing U-bend joint with pipes. Each loop was attached with 90 degree bend at the top with extension pipes for future connections. Loops were pressure tested for any leakage in the connection after construction. These pipes were filled with water and sealed with cap at both outlets and then attached to the circumference of reinforcement cage. Filled water in the pipes helps to prevent the damage during pouring of concrete. Pipes loops fitted in the reinforcement cage are shown in Figure 3-2.

a. b.

Figure 3-2: Heat exchanger pipes a) u-shape bend at bottom side, b) Closed pipes with extension pipes at top

Based on the experience gained from previous work, it is advised to use wider U-shaped bend and it is better to leave straight extension pipes rather than making a 90 degree bend extension for ease of work.

Vibrating Wire Strain Gauges

Geokon vibrating wire rebar strain meters (Figure 3-3) were used for the monitoring the temperature and the strain changes in the center of the pile. These sensors were equipped with high strength steel and were designed to tie parallel to structural reinforcement bar. These sensor are reliable and easy to install, and use and also their readings are unaffected by moisture and cable length. Temperatures were recorded in degree Celsius and strains were measured in terms of digits unit. Digit unit is converted to micro strain by multiplying with a calibration factor (C) of each specific sensors provided by manufacturer. Digits were converted to actual micro strain from following relations;

$$\varepsilon_{actual} = (R_1 - R_0) * C + (T_1 - T_0) * K_{steel}$$

where, R_1 = current recorded digits, R_0 = initial recorded digits at start of test, T_1 = current temperature, T_0 = initial temperature at start of test, C= calibration factor, and K_{steel} = expansion coefficient of steel (12.2 ppm/°C).

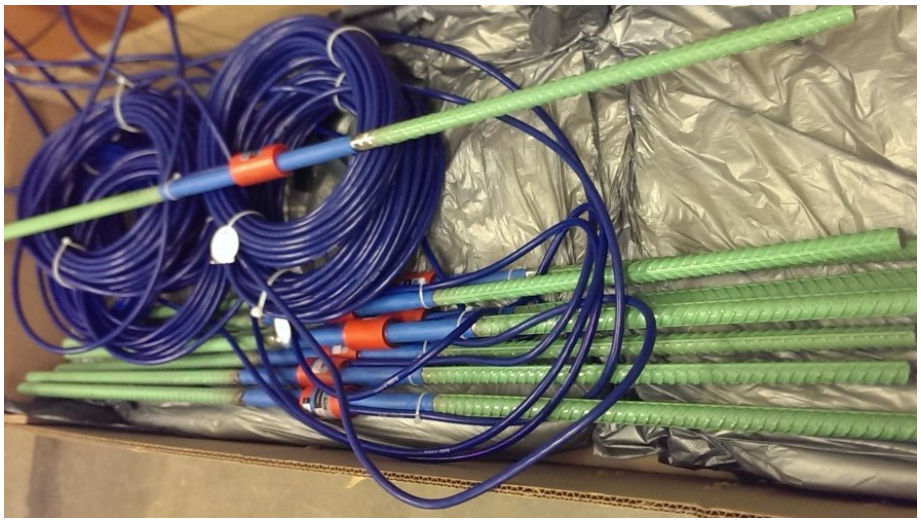

Figure 3-3: Vibrating wire gauge

Heat Injection (Thermal Response Test) Device

Heat injection into the ground by circulating heat exchanger fluid in heat exchanger pipes was carried out by using the trailer constructed in Oklahoma state university (Austin 1998). This experimental trailer was developed for the measurement of ground thermal properties by running TRT in the borehole. It comprises single axle trailer as shown in Figure 3-4. It contains all necessary equipment to conduct the test: water heating element, water supply/purging tank, pump, flow-meter, temperature measuring sensors, generator, and data logging equipment. Water supply system, power supply system, heating system, and temperature and flow measurement system all were equipped inside the trailer. Detailed information about construction and operation is available in Austin (1998).

Figure 3-4: Heat injection trailer

Data logger

For the measurement of strain and temperature in the center of the pile at eight different depths, vibrating wire strain gauges were used. Data were recorded using Campbell CR1000 data loggers (Figure 3-5). Figure 3-5 shows the connection of wires to the data logger. Desired data logging interval can be set up. Large amount of data can be stored in data logger which is also equipped with battery backup for any breakage in power supply.

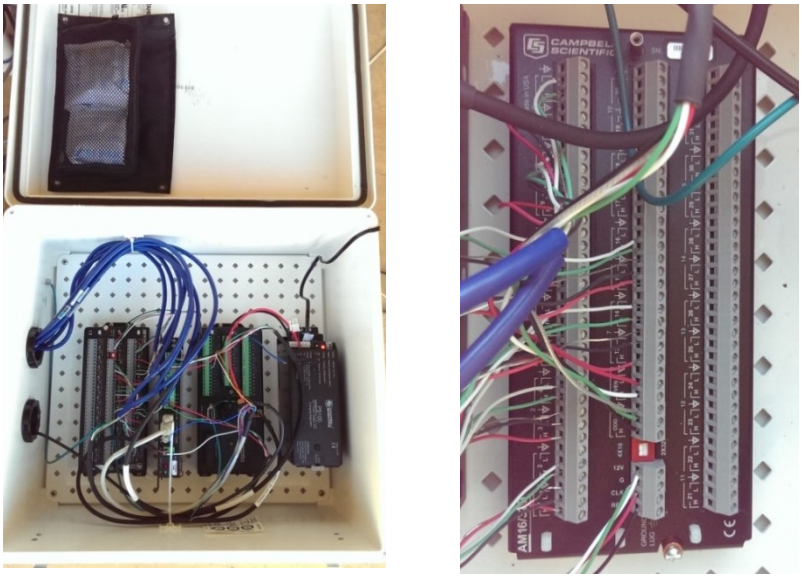

a. b.

Figure 3-5: Data logger setup a) Data logger, b) Sensor connections

Other Setup

All pipes exposed at top were insulated with foam insulation, and then covered by plastic for preventing from rain. Whole structure was covered by garden shed (Figure 3-6) for protection. Power to both the trailer and the data logger setup was supplied from the nearby building. No power outage or shortage occurred during the experiment.

Figure 3-6: Final experimental setup

3.2 EXPERIMENTAL PROCEDURE

This section provides the soil profile information and the pile test procedure.

3.2.1 SOIL EXPLORATION

Site exploration was conducted by a 4.5-inch drill auger l with standard penetration test (SPT), and Texas cone penetration test (TCP) and soil samplings.

SPT and TCP Results

The boring log (Figure 3-7) shows that ground comprises soft clay to hard dense shale. The whole soil profile (depth of interest 40 feet) can be viewed as 2 layers: top layer of soft clay up to 10 feet and below that shale formed from clay consolidation. Lower portion of second layer below 30 feet was found to be very dense, only penetration of 0.1 to 2.5 inch in 50 blows was achieved with the Texas cone penetrometer. No caving was observed in the hole during boring; proofing soil to be very stiff.

Laboratory Tests

Sample obtained from the auger boring were tested for soil identification and classification. Very few samples were obtained as most part of the surface was very hard and stiff making impossible to use the SPT sampler. Five samples were obtained at different depth (mostly from above 10 feet). They were tested for water content, liquid limit, and plastic limit. Results obtained were listed in Table 3-1.

Table 3-1: Laboratory tests results

Depth	Sample Type	Liquid Limit	Plastic Limit	Plasticity Index	Soil Type
0 feet	SPT	54	21	33	Fat Clay
4 feet	SPT	29	16	13	Lean Clay
7 feet	SPT	26	16	10	Sandy Lean Clay
10 feet	SPT	27	13	14	Lean Clay
25 feet	SPT	43	17	26	Shale

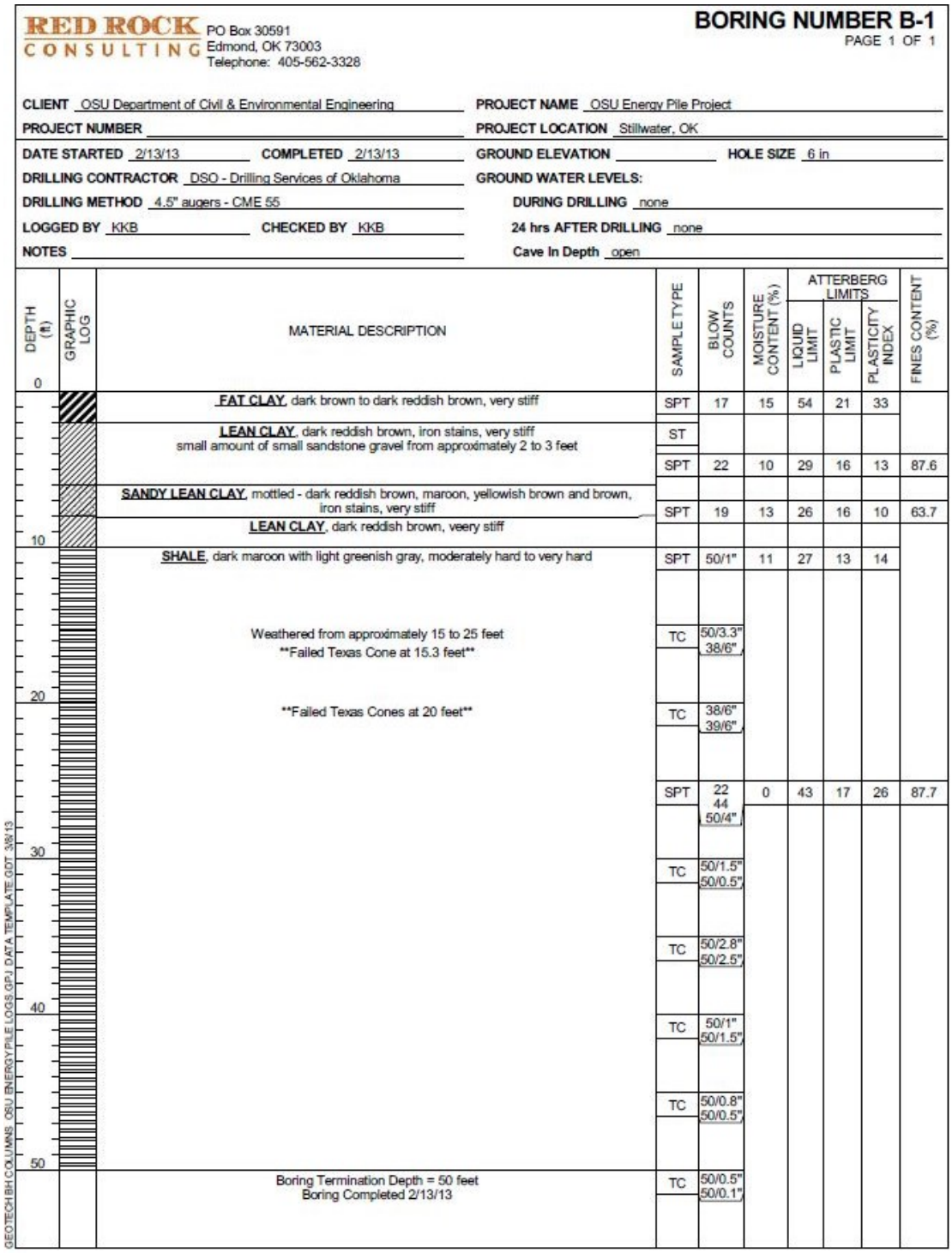

RED ROCK CONSULTING
PO Box 30591
Edmond, OK 73003
Telephone: 405-562-3328

BORING NUMBER B-1
PAGE 1 OF 1

CLIENT OSU Department of Civil & Environmental Engineering
PROJECT NAME OSU Energy Pile Project
PROJECT NUMBER
PROJECT LOCATION Stillwater, OK
DATE STARTED 2/13/13 **COMPLETED** 2/13/13
GROUND ELEVATION **HOLE SIZE** 6 in
DRILLING CONTRACTOR DSO - Drilling Services of Oklahoma
GROUND WATER LEVELS:
DRILLING METHOD 4.5" augers - CME 55
DURING DRILLING none
LOGGED BY KKB **CHECKED BY** KKB
24 hrs AFTER DRILLING none
NOTES
Cave In Depth open

DEPTH (ft)	GRAPHIC LOG	MATERIAL DESCRIPTION	SAMPLE TYPE	BLOW COUNTS	MOISTURE CONTENT (%)	ATTERBERG LIMITS: LIQUID LIMIT	ATTERBERG LIMITS: PLASTIC LIMIT	ATTERBERG LIMITS: PLASTICITY INDEX	FINES CONTENT (%)
0		**FAT CLAY**, dark brown to dark reddish brown, very stiff	SPT	17	15	54	21	33	
		LEAN CLAY, dark reddish brown, iron stains, very stiff small amount of small sandstone gravel from approximately 2 to 3 feet	ST						
			SPT	22	10	29	16	13	87.6
		SANDY LEAN CLAY, mottled - dark reddish brown, maroon, yellowish brown and brown, iron stains, very stiff	SPT	19	13	26	16	10	63.7
10		**LEAN CLAY**, dark reddish brown, veery stiff							
		SHALE, dark maroon with light greenish gray, moderately hard to very hard	SPT	50/1"	11	27	13	14	
		Weathered from approximately 15 to 25 feet **Failed Texas Cone at 15.3 feet**	TC	50/3.3" 38/6"					
20		**Failed Texas Cones at 20 feet**	TC	38/6" 39/6"					
			SPT	22 44 50/4"	0	43	17	26	87.7
30			TC	50/1.5" 50/0.5"					
			TC	50/2.8" 50/2.5"					
40			TC	50/1" 50/1.5"					
			TC	50/0.8" 50/0.5"					
50									
		Boring Termination Depth = 50 feet Boring Completed 2/13/13	TC	50/0.5" 50/0.1"					

GEOTECH BH COLUMNS - OSU ENERGY PILE LOGS.GPJ DATA TEMPLATE.GDT 3/8/13

Figure 3-7: Boring log of project site

3.2.2 HEAT EXCHANGER PIPES CONNECTION

Eight U-shaped heat exchanger pipes were installed in the bored pile. A total of 16 pipe outlets were present at the top of the pile. Heat exchanger fluid (water) can be circulated in many ways through these pipes. All 8 loops can be connected in series or parallel connection can be made. Finally it was decided to make two series connection of each 4 loops and a making parallel connection of these two series connection as shown in Figure 3-8. Before the connection was made each loop was pressure tested to check if any breakage and leakage had happened during concrete pouring. All loops were found to be intact. The connections were made as shown in Figure 3-8. Final pipe configuration after connection is shown in Figure 3-9. After series and parallel connections were made, all exposed pipes were insulated with foam insulation. Pipes were fully covered to minimize the heat loss to the atmosphere during the test (Figure 3-9). Then all pipes were covered with plastic to prevent wetting of insulation foam from rain. Finally the whole setup was covered with a garden shed (Figure 3-9).

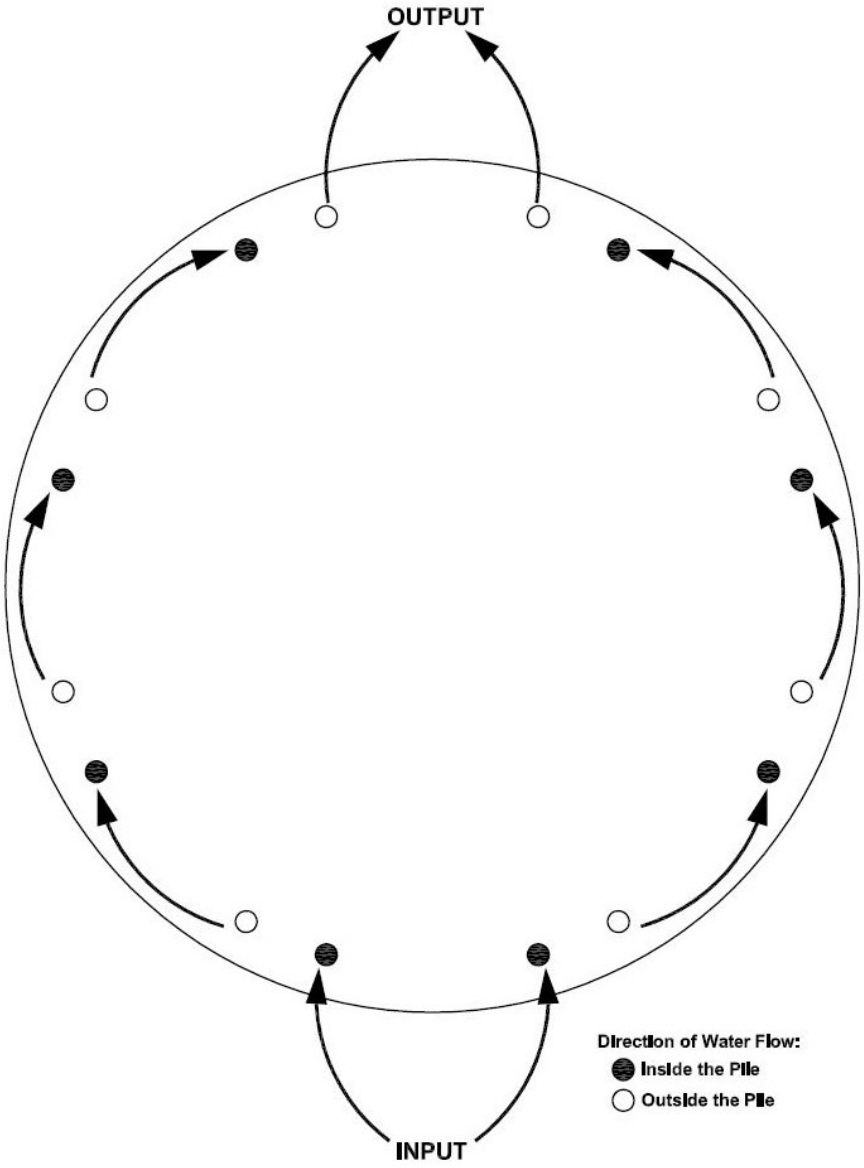

Figure 3-8: Pipes connection layout

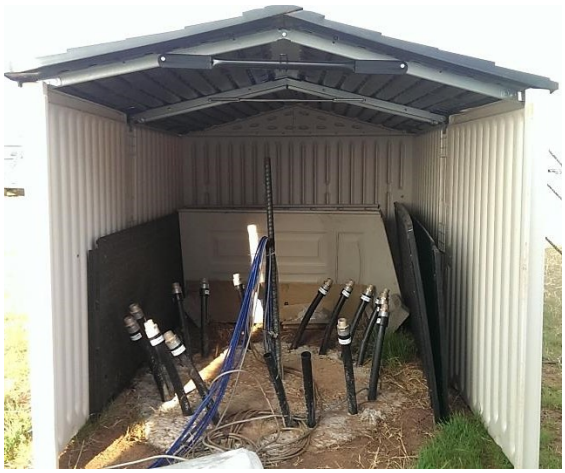




Figure 3-9: Steps of pipe connection

CHAPTER 4

THERMAL RESPONSE TEST RESULTS

4.1 INTRODUCTION

A thermal response test was conducted on the pile. The inlet and outlet flow temperatures were measured during the test. In addition to the flow rate, changes in the pile temperature, and axial strains developed in the pile were also measured. Test was run for 39 days to achieve an appreciable increase in both the flow and the pile temperature. At the end of the test, the pile temperature was 35.4° C, and the mean flow temperature was 37.1° C. Table 4-1 summarizes key facts of the test.

Table 4-1: Summary of Test

Start of Test	May, 15, 2014
End of Test	June, 23, 2014
Duration of test	39 days
Pile Diameter (m)	1.067 m
Pile Length (m)	12.2 m
Heat Exchanger Pipes Configuration	8 U-loop
Water Flow Rate	0.38 liter/sec
Constant Heat Supply	2000 W
Initial Mean Flow Temperature	17.21°C
Final Mean Flow Temperature	37.14°C
Initial Mean Pile Center Temperature	16.06°C
Final Mean Pile Center Temperature	35.38°C

4.2 COLLECTED DATA

Following section provides details about different collected data during the test.

4.2.1 HEAT FLOW

A constant heat of 2000 Watt was supplied to the pile during the test. Heating of water at a constant rate was achieved by the heater element present in the trailer. Figure 4-1 shows measured and targeted heat flow rate. The maximum supplied heat was 2100.77 W, the minimum was 1889.85 W, and the average was 2002.22 W. A small variation was seen in the targeted heat flow rate, but considering the length of the test the overall heat supply can be considered uniform.

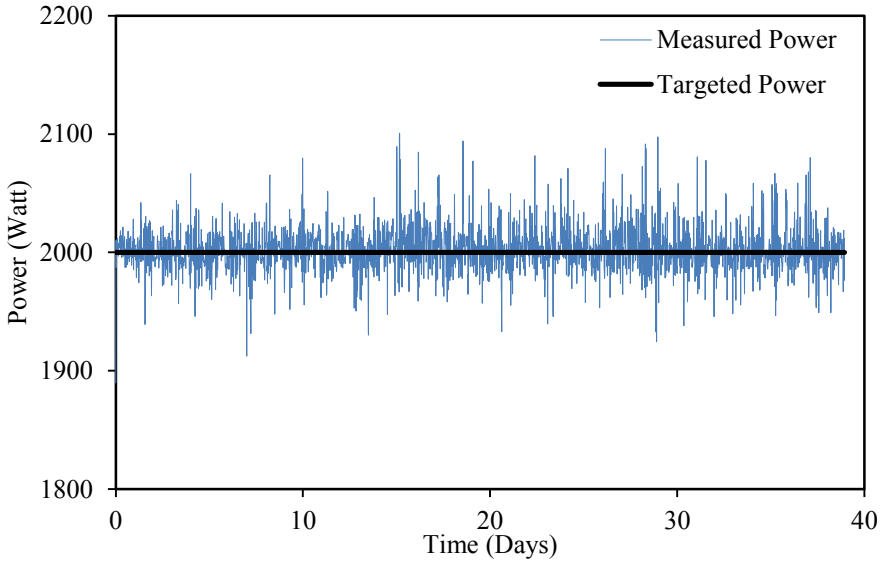

Figure 4-1: Heat flow rate during test

4.2.2 WATER FLOW RATE

A constant flow rate of 0.38 liter/sec (heat exchanger fluid: water) was maintained during the test. A flowmeter was used to record the flow rate. The flow rate was selected for

increasing the heat transfer by creating turbulent flow in the pipe. Actual and the targeted flow rate was shown in Figure 4-2. The mean flow rate and variation in the Reynolds number are also shown in Figure 4-3. Maximum, minimum, and average flows were 0.3826 liter/sec, 0.3773 liter/sec, and 0.3803 liter/sec respectively. Flow rate was almost constant at desired rate; there was no significant deviation in the flow rate.

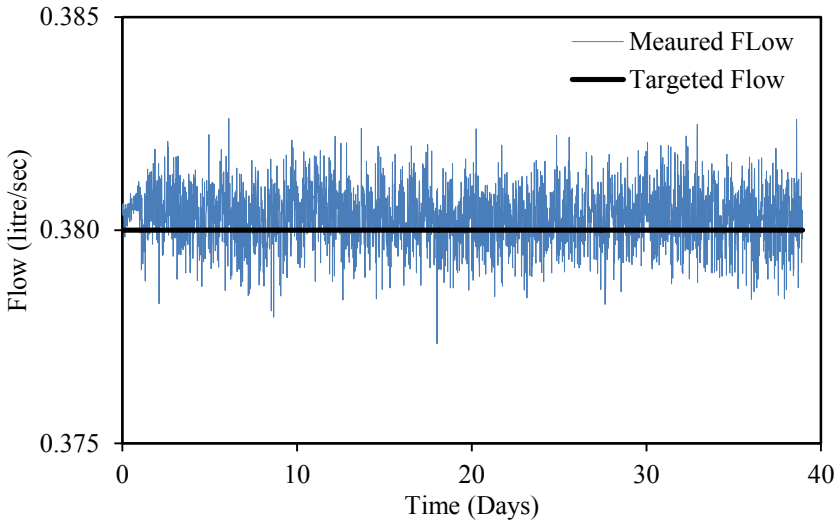

Figure 4-2: Flow rate during the test

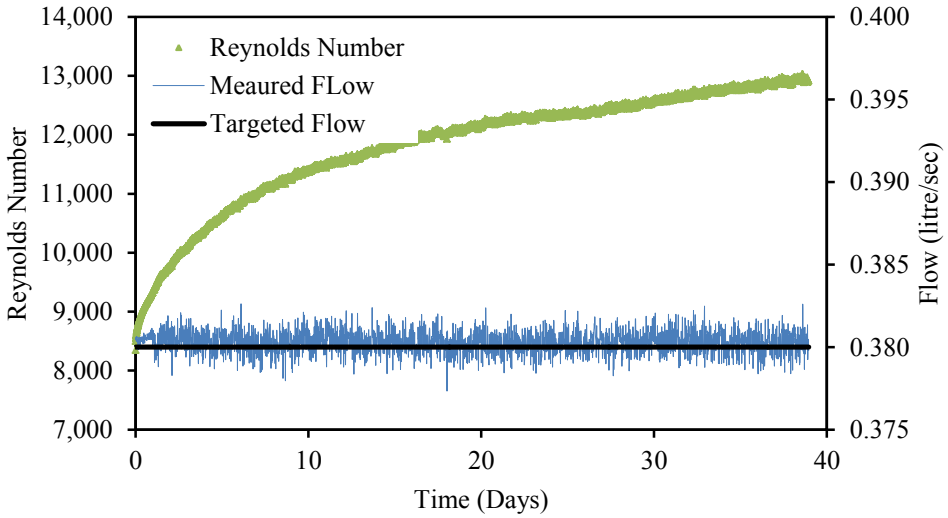

Figure 4-3: Variation of Reynold's number with flow during test

4.2.3 INFLOW/OUTFLOW TEMPERATURE

The inflow and outflow temperature were recorded during the test. Continuous increase of inflow and outflow temperature was observed. Inflow/outflow and the mean flow temperature are shown in Figure 4-4.

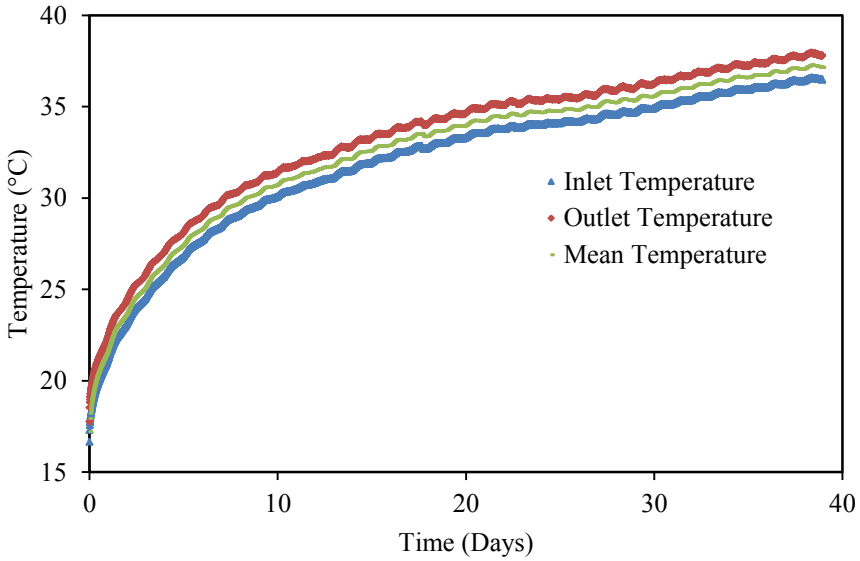

Figure 4-4: Inflow/outflow temperature

4.2.4 PILE CENTER TEMPERATURE

The pile temperature variation along the center of the pile during the test was recorded using the built-in thermistors in the strain gauges. The variation of the temperature along the length of pile at different depth is shown in Figure 4-5. It is shown that the rate of pile temperature rise at various depths was relatively uniform except at lowest depth which had relatively lower temperature rise. Figure 4-6 shows the variation of temperature at different depth of the pile with time.

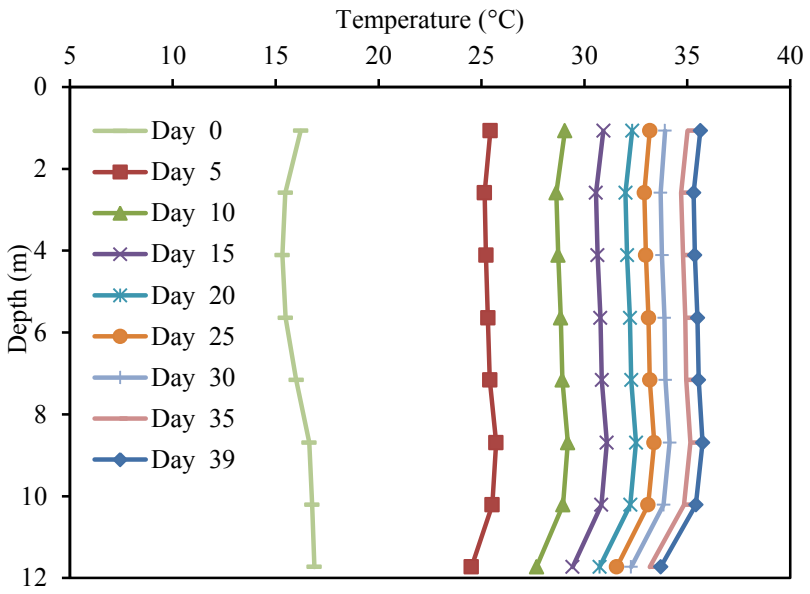

Figure 4-5: Pile center temperature at different depth in different time during testing

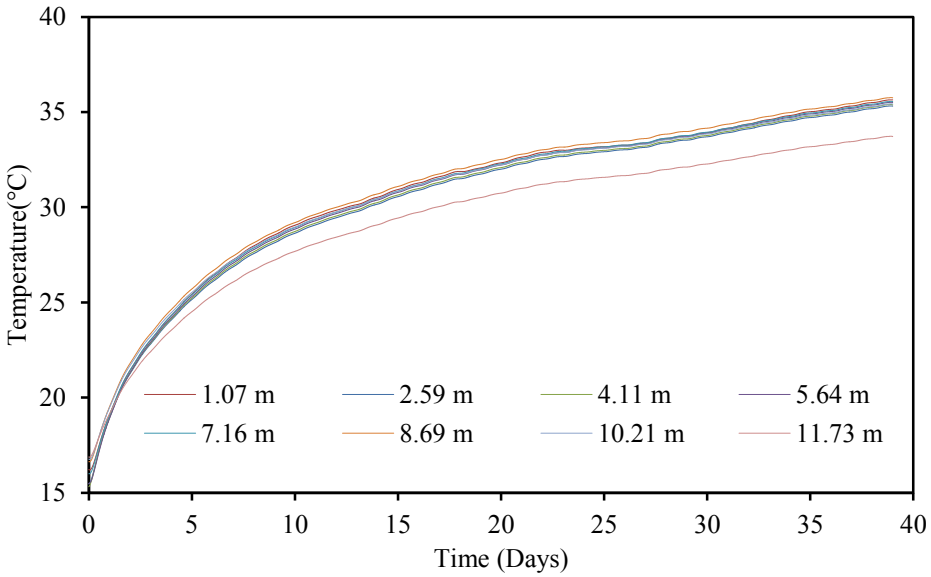

Figure 4-6: Variation of pile center temperature with time at different depths

4.2.5 AXIAL STRAIN AT CENTER OF PILE

The axial strain at the center of the pile was recorded using eight strain gauges installed on the center rebar at different depths of the pile. A sample calculation of the strain at

5.64 m (18.5 feet) depth when the temperature of pile increased by 10° C is shown below. The compressive strain is considered as positive.

$$\varepsilon_{actual} = -((R_1 - R_0) * C + (T_1 - T_0) * K_{steel})$$

where R_1 = 2607 digits T_1 = 26.2°C

R_0 = 2624 digits T_0 = 16°C

C = 0.349 µstrain per digits

K = 12.2 ppm/°C

$$\varepsilon_{actual} = -(2607 - 2624) * 0.349 - (26.2 - 16) * 12.2$$

$$\varepsilon_{actual} = -118.5 \text{ µstrain}$$

Figure 4-7 shows the measured strain at different depths of the pile at different time. These strains were not at the same thermal load as changes in temperature at different depth were different. Figure 4-8 shows changes in strain with time in different depth of the pile.

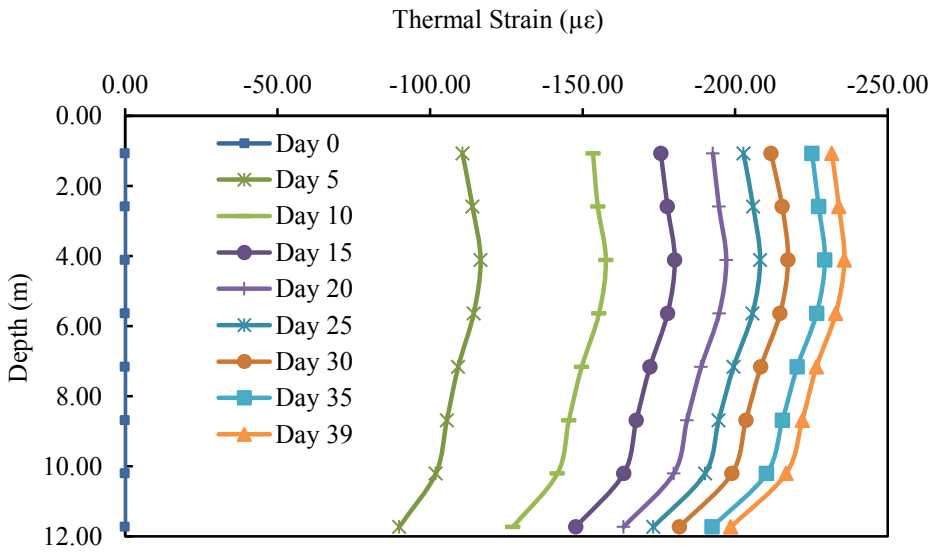

Figure 4-7: Measured pile center thermal strain at different depth in different time during testing

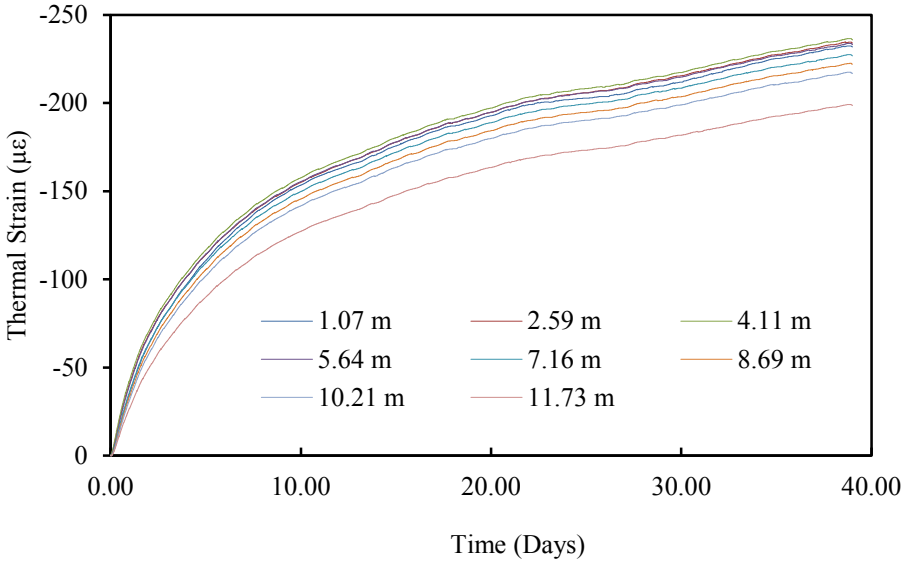

Figure 4-8: Variation of pile center thermal strain with time at different depths

CHAPTER 5

ANALYSIS AND DISCUSSION

5.1 TEMPERATURE VARITION IN PILE

Table 5-1 shows the variation of temperature along the centerline of the pile from the start of the test. These temperatures were recorded at the same time of the day. Day 0 temperature represents the undisturbed ground temperature and all other temperatures are resulted from the of heat injection during the test.

Table 5-1: Temperature variation in center of pile

Depth (m)	Temperature (°C) in days from start of test								
	Day 0	Day 5	Day 10	Day 15	Day 20	Day 25	Day 30	Day 35	Day 39
1.07	16.22	25.43	29.05	30.93	32.33	33.18	33.92	35.02	35.64
2.59	15.47	25.15	28.63	30.56	32.00	32.92	33.7	34.71	35.31
4.11	15.32	25.22	28.73	30.64	32.08	32.99	33.77	34.79	35.37
5.64	15.48	25.31	28.85	30.78	32.22	33.12	33.89	34.90	35.5
7.16	16.00	25.41	28.93	30.85	32.28	33.18	33.94	34.95	35.55
8.69	16.63	25.71	29.19	31.09	32.51	33.39	34.15	35.16	35.75
10.21	16.77	25.52	28.96	30.83	32.23	33.1	33.85	34.84	35.42
11.73	16.88	24.51	27.68	29.43	30.74	31.57	32.27	33.18	33.71
Avg.	16.10	25.28	28.75	30.64	32.05	32.93	33.69	34.69	35.28

The average pile center temperatures at different depths were calculated for all recorded temperature data. Then the average increases of temperature from the Day 0 temperature (16.10° C) were calculated. The average increase of the pile center temperature with time is shown in Figure 5-1.

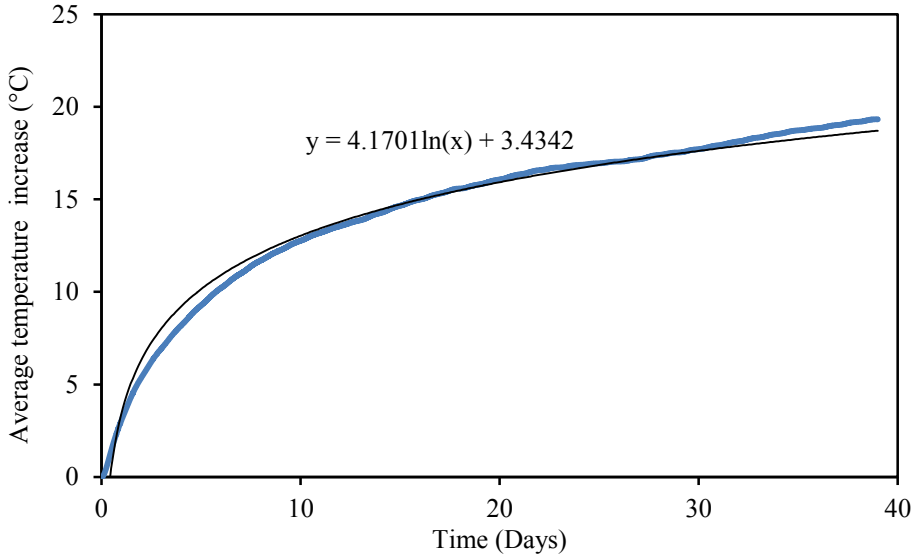

Figure 5-1: Average temperature increase of pile center with time

The best fit curve was presented in Figure 5-1. Based on the fitted curve, the change in the pile temperature over a different period of time was approximated. Table 5-2 shows the change in temperature of the pile at the end of one month (30 days), three months (90 days), and six months (180 days).

Table 5-2: Average pile temperature increase at different time

Time (Days)	30	90	180
Temp^{r} (°C)	17.62	22.2	25.09

The change in pile temperature was about 25° C for six months continuous heat supply (2000 W). In real GHX-pile operation, heat extraction and injection cycle changes seasonally (winter and summer). This reversal process helps to regain a balanced ground (or pile) temperature without overheating or overcooling of the pile. The heat injection amount varies from daily average load to peak load during operation. Therefore, based on these facts, it can be concluded that the thermal load (change of temperature) in bigger pile in similar soil condition will not exceed 25 °C to 30 °C during heat injection (cooling cycle) process. In the current study applied thermal load in pile was 20°C.

5.2 THERMAL STRAIN

The GHX pile tends to expand with the temperature increase, and a thermal strain was developed. If the expansion is restricted by surrounding soil, thermal stress is developed. The observed thermal strains at different depths were plotted with the temperature change at corresponding locations as shown in Figure 5-2. Here compressive strains were considered as positive. The slope of each curve was used to calculate the coefficient of thermal expansion of the pile at each respective depth. The calculated values are listed in Table 5-3. The observed coefficients of thermal expansion were less than free expansion coefficient due to the restriction of the surrounding soil.

As there was no head load or any other restriction in head movement and also soil restriction was less in the top part, coefficient of expansion obtained from the top sensor should be close to the free expansion coefficient of the concrete pile. The calculated value of thermal expansion coefficient of top sensor was 11.907 $*10^{-6}$/°C, so free thermal

expansion coefficient of installed concrete pile was predicted to be $12*10^{-6}$/°C. This value is within the typical range ($7*10^{-6}$/°C to $13*10^{-6}$/°C) provided by FHWA (2014) for concrete's thermal expansion coefficient.

Table 5-3: Calculated coefficient of thermal expansion of pile at different depth

Depth (m)	Coefficient of thermal expansion of pile (10^{-6}/°C)
1.07	11.907
2.59	11.811
4.11	11.768
5.64	11.677
7.16	11.602
8.69	11.618
10.21	11.626
11.73	11.796

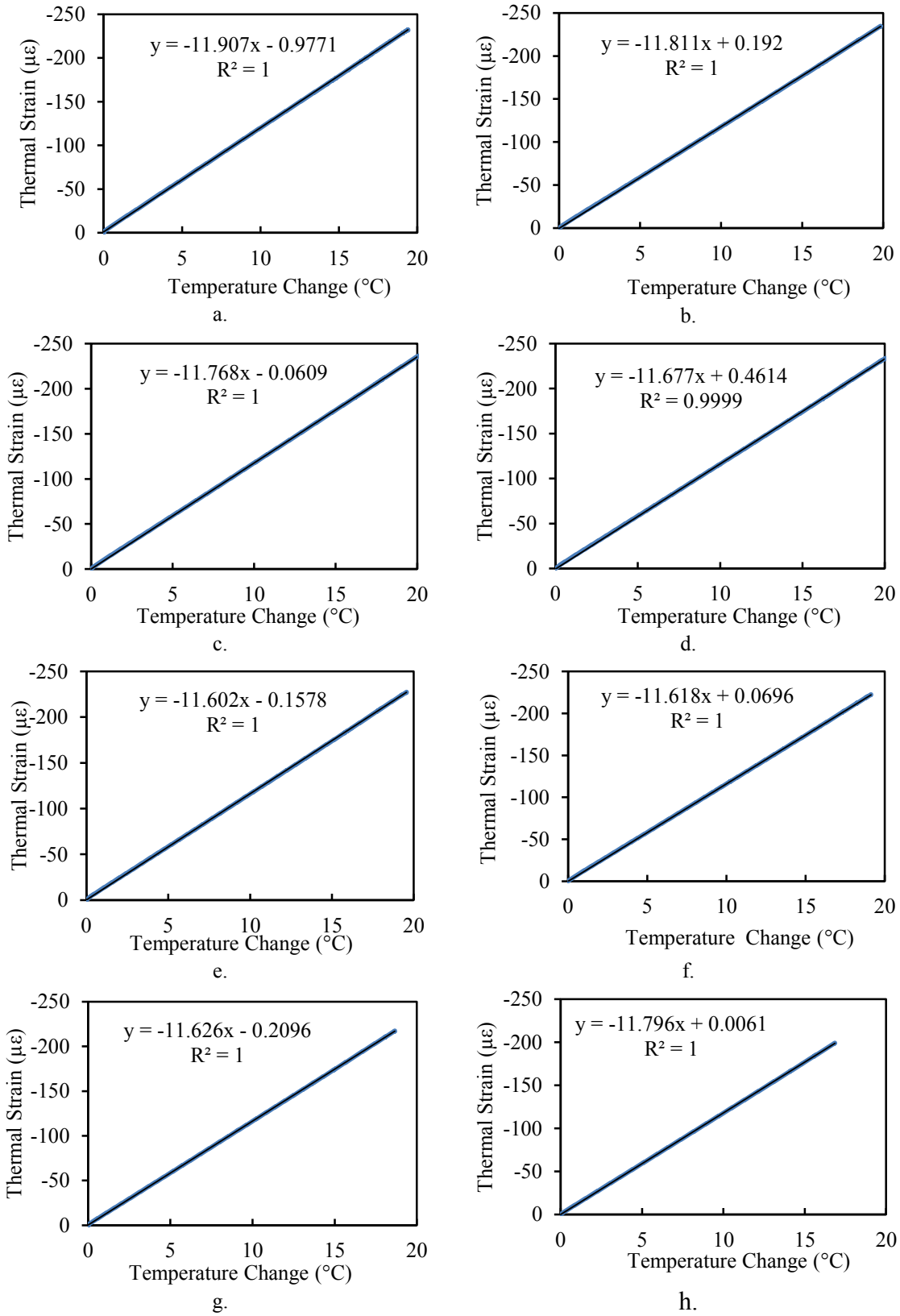

Figure 5-2: Thermal strain vs change in temperature at different depth: a) 1.07 m, b) 2.59 m, c) 4.11 m, d) 5.64 m, e) 7.16 m, f) 8.69 m, g) 10.21 m, and h) 11.73 m

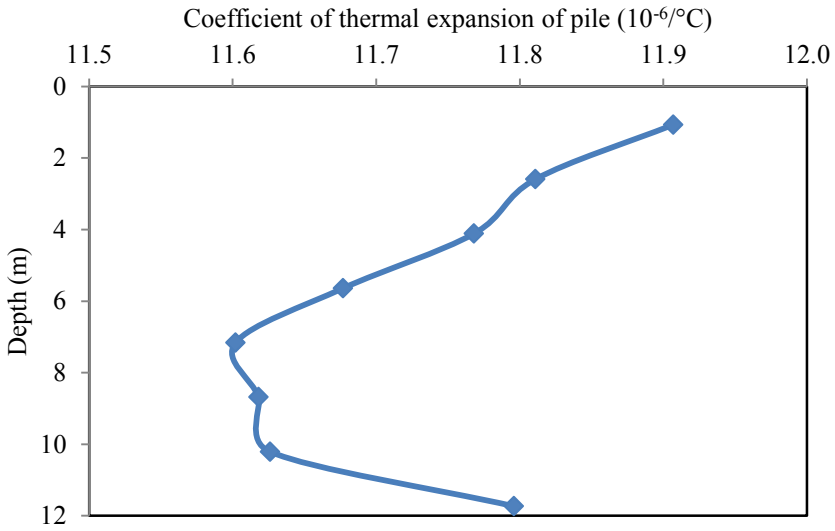

Figure 5-3: Variation of coefficient of thermal expansion of pile with respect to depth

Figure 5-3 shows the variation of calculated thermal expansion coefficient of the pile at various depths. The maximum value was obtained at the top and it decreased with depth till it reached the least value around the mid of the pile. With the increase of depth, soil side resistance in the pile increases; this restricts expansion of the pile, resulting in a lower value of expansion. During heating, the top half portion of the pile tended to move up, and the lower half tended to move down. This variation implies more soil restriction in the middle portion of the pile and less in top and bottom section.

Observed thermal strains in the GHX-pile during testing at different thermal load are listed in Table 5-4. At any instance the directly measured strain distribution in the pile (as shown in Figure 4-7) was different than listed in Table 5-4 because the temperature of the pile was not the same along the length (as shown in Figure 4-6). Therefore, the directly measured strain distribution at any instance in different depth of the pile was due to the

different thermal load. For better understanding of thermal behavior of the GHX-pile, strain distribution was obtained assuming uniform thermal load along the pile. Observed strain at different thermal load at each depth was obtained from strain vs temperature distribution curve (Figure 5-2).

Table 5-4: Observed thermal strain at different thermal loading

Depth (m)	Observed strain (10^{-6}) at thermal load (°C) of								
	Δ1.00	**Δ2.50**	**Δ5.00**	**Δ7.50**	**Δ10.00**	**Δ12.50**	**Δ15.00**	**Δ17.50**	**Δ19.30**
1.07	-12.88	-30.74	-60.51	-90.28	-120.05	-149.81	-179.58	-209.35	-230.78
2.59	-11.62	-29.34	-58.86	-88.39	-117.92	-147.45	-176.97	-206.50	-227.76
4.11	-11.83	-29.48	-58.90	-88.32	-117.74	-147.16	-176.58	-206.00	-227.18
5.64	-11.22	-28.73	-57.92	-87.12	-116.31	-145.50	-174.69	-203.89	-224.90
7.16	-11.76	-29.16	-58.17	-87.17	-116.18	-145.18	-174.19	-203.19	-224.08
8.69	-11.55	-28.98	-58.02	-87.07	-116.11	-145.16	-174.20	-203.25	-224.16
10.21	-11.84	-29.27	-58.34	-87.40	-116.47	-145.53	-174.60	-203.66	-224.59
11.73	-11.79	-29.48	-58.97	-88.46	-117.95	-147.44	-176.93	-206.42	-227.66

The variation of the observed thermal strain at 10° C thermal load is shown in Figure 5-4 (a) and the corresponding compressive stress developed in soil is shown in Figure 5-4 (b). At the upper level, the pile expanded more, nearly equal to free expansion, because there was no head load and also there was less soil restriction. At the top surface, the pile expansion was free, so no stress was developed. With the increase in depth, the soil side friction increases, this restricts the movement of the pile, so less strain was developed. The minimum axial strain was obtained around the middle of the pile below which strain again starts to increase towards the bottom. The highest compressive stress of soil was observed in the location of the minimum axial strain in the pile.

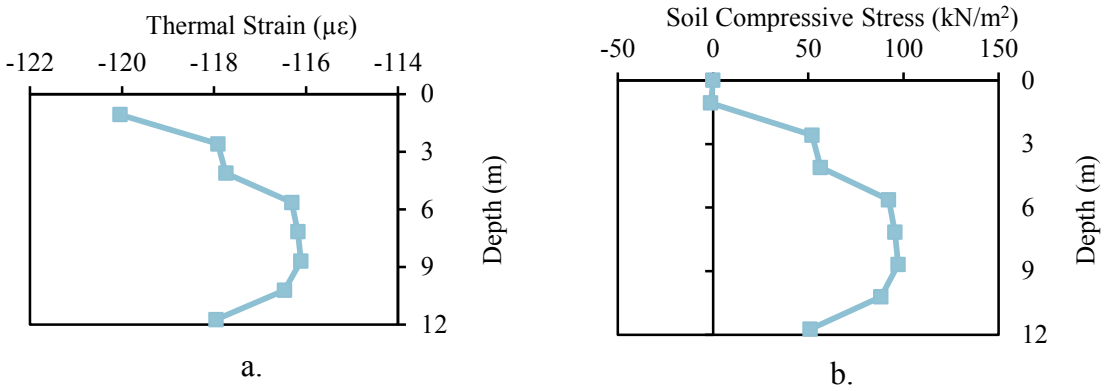

Figure 5-4: a) Observed strain at thermal load of 10° C and b) Soil compressive stress developed at thermal load of 10° C

Figure 5-5 shows the variation of the induced soil compressive stress along the length of the pile at different thermal load. Compressive stress increases with the increase in the thermal load. The maximum value of compressive stress was observed in the middle of the pile in all thermal loading. Figure 5-5 shows that more side resistance was mobilized with the increase in thermal loading. The maximum compressive stresses were within the limit of soil capacity.

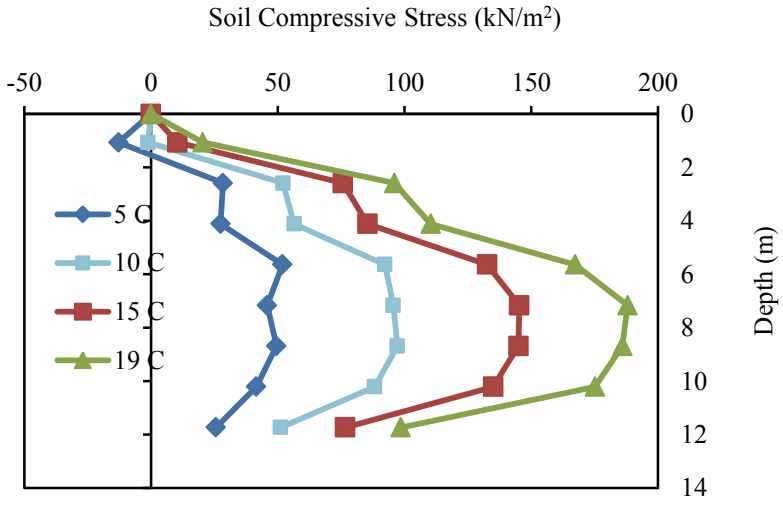

Figure 5-5: Variation of soil compressive stress with different thermal load

5.3 THERMAL ANALYSIS (THERMAL RESPONSE TEST)

The recorded inflow, outflow, and the mean temperature of heat exchanger fluid are presented in Figure 5-6. The initial rate of temperature rise was high because initially water was at the room temperature and water takes initial supply of the heat. Heated water starts to emit heat to the ground when water temperature becomes more than the ground (pile) temperature. Due to the transmission of heat from the heat exchanger fluid to the surrounding mean temperature of fluid increases slowly.

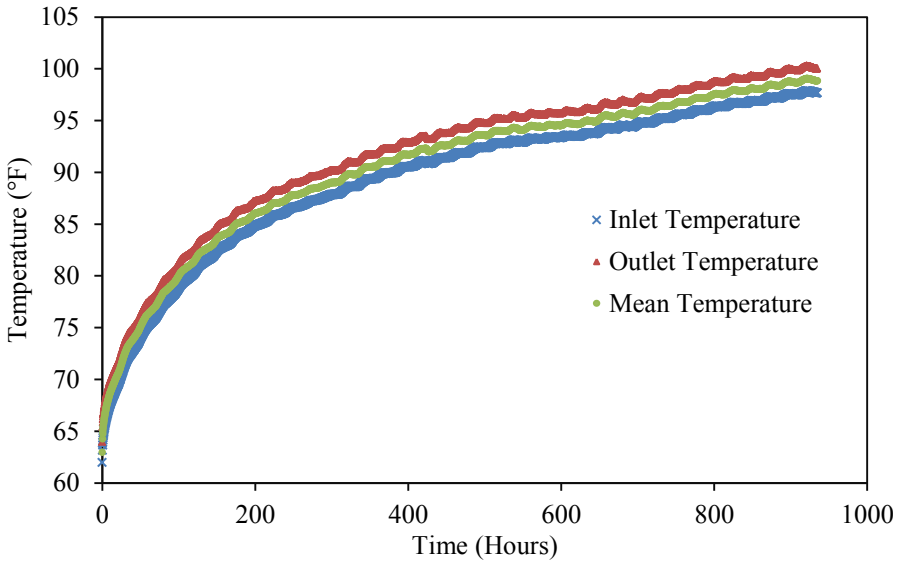

Figure 5-6: Heat exchanger fluid temperature variation

Line Source Model

The thermal response test data were analyzed using the line source model theory. The test had been run for a considerably longer period of time, so the line source model may give good result in estimation of ground thermal properties. Test was run for a total of 936 hours. Considering ground diffusivity of $5.4*10^{-7} m^2/s$ for clay (Table 2-1). Time duration ($5r^2/\alpha$) was proposed by Eskilson (1987) for disregarding initial data (based on radius

of the pile and thermal diffusivity of soil) before applying line source model in test data. In current condition it gives 730 hours duration up to which observed data were neglected. The slope was calculated from the remaining data by fitting logarithmic trendline as shown in Figure 5-7.

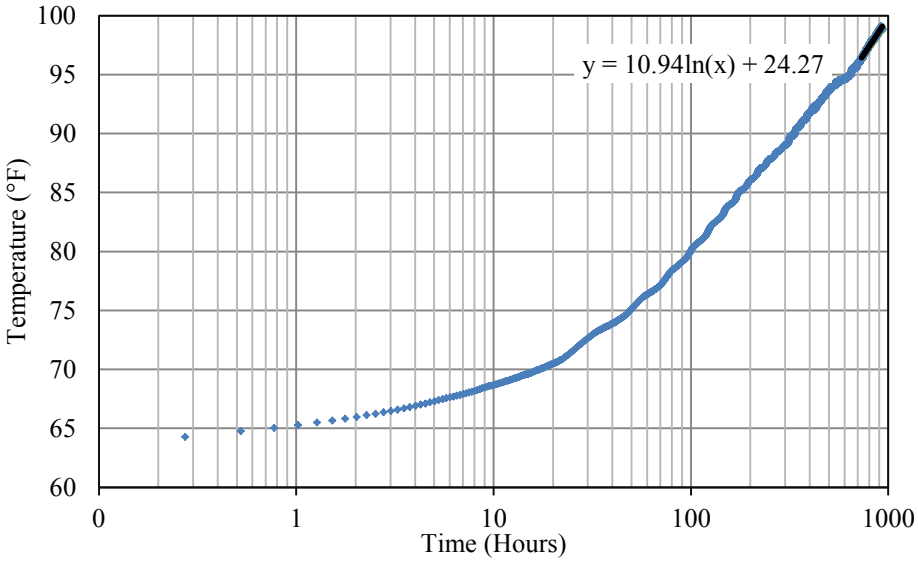

Figure 5-7: Slope of data after 730 hour

The thermal conductivity of the ground from the rest of data was calculated using the following relationship:

$$K = \frac{Q}{4\pi * Slope * L}$$

where, Q = 6824.28 Btu/hr

L = 40 ft

$$K = \frac{6824.28}{4\pi * 10.94 * 40} = 1.24 \text{ Btu/hr} * \text{ft} * \text{F}$$

The calculated value was higher than typical values given in Table 2-1 for clay soil, but the soil profile has shale in most portion of the pile, which justifies the higher thermal

conductivity. Shale has higher thermal conductivity in the range of 1 to 4 $\mathrm{Btu/hr} * \mathrm{ft} * \mathrm{F}$. Figure 5-7 shows data after 100 hours has same linear trend of increase in temperature. So different trendlines were fitted considering data after 100 hours for checking variation in result with amount data considered. The end point of each set of data was kept constant while different start points (100, 200, 300, 400, 500, 600, 700, and 800 hours) were selected. Slope of each considered data were calculated (Figure 5-8). Calculated thermal conductivity is shown in Table 5-5.

Table 5-5: Thermal conductivity with different length of data

Start time of data (hr)	Slope from plot	Thermal conductivity (Btu/hr*ft*F)
100	8.29	1.64
200	8.32	1.63
300	8.37	1.62
400	8.42	1.61
500	9.04	1.50
600	10.69	1.27
700	11.13	1.22
730	10.94	1.24
800	10.20	1.33

Up to 500 hours thermal conductivity were in the range of 1.60 to 1.65 Btu/hr*ft*F but after that it lowers in range of 1.2 to 1.3 Btu/hr*ft*F. Result were not consistent but are within the given range of typical values for shale. This little variation in calculated values may be due to the large thermal capacity of concrete pile which was not considered in this model. Also pile has large diameter, which allow transmission of heat in axial direction also, not only in the radial direction.

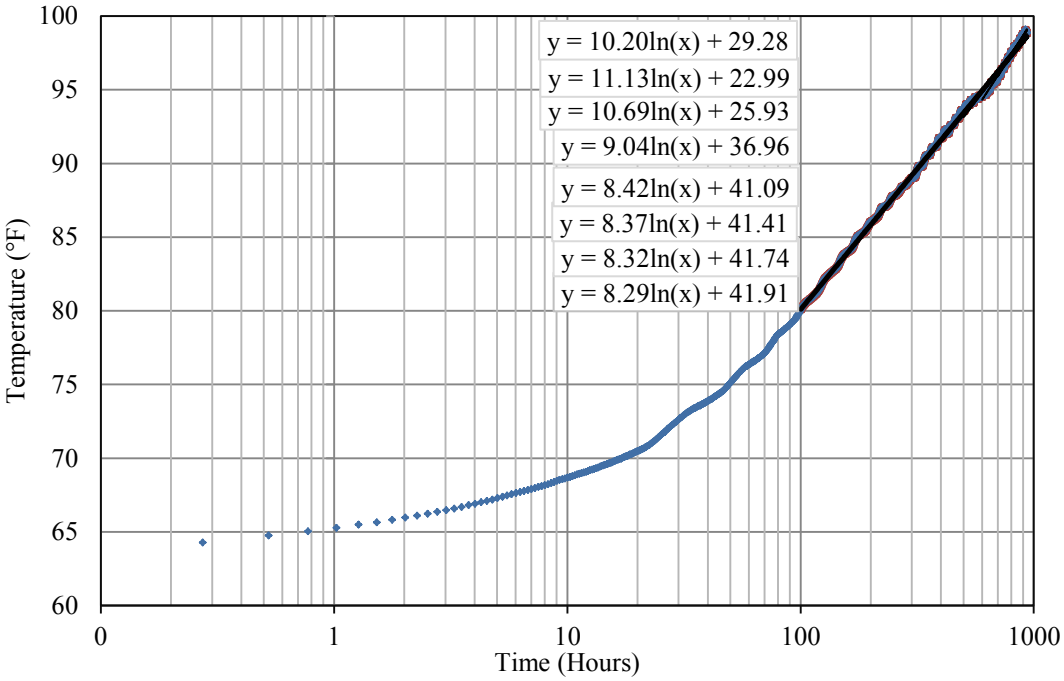

Figure 5-8: Slope of various set of data after 100 hour

5.4 LOAD-DISPLACEMENT (t-z) MODEL FOR GHX-PILE

As explained earlier Knellwolf et al. (2011) used load-transfer concept on analyzing displacement induced in the GHX-pile by mechanical and thermal loading. In the current study, the development of modified load-displacement model based on the t-z model described in (Reese et al. 2006) was done by introducing the temperature effect in the model. Basic assumptions made during development of the model were:

- Properties of the pile such as Young's modulus (E), coefficient of thermal expansion (α_{pile}), and cross sectional area (A) remain constant along the length of pile.
- Soil does not expand or contract with the temperature change.
- Soil properties remain constant in each layer and will not change with change in temperature. The load transfer coefficients of each layer are known and constant.
- Only axial displacement of the pile is considered, radial displacement is considered negligible.
- The temperature along the pile length is uniform.
- No water table is present; effect of moisture migration is neglected.

Downward displacement and compressive force are considered positive. The pile was discretized into small segments (as shown in Figure 5-9) with length dx and axial force P. Each segment undergoes displacement z at depth x from the top.

For each pile element,

$$\frac{dz}{dx} = -\frac{P}{EA}$$

$$P = -EA\frac{dz}{dx} \quad (1)$$

where, P = axial force in the pile, E = Youngs modulus of the pile, A = cross sectional area of the pile

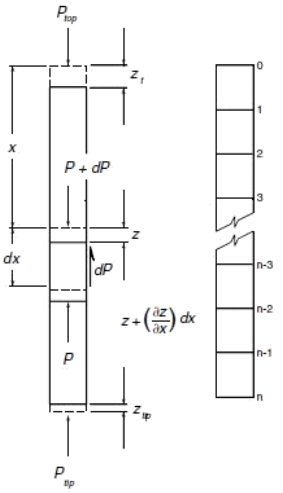

Figure 5-9: Discretization of axially loaded pile (Reese et al. 2006)

When thermal load of ΔT is presented, the total axial force becomes:

$$P = -EA\frac{dz}{dx} + \Delta T\alpha_{pile}EA \quad (2)$$

where, ΔT = change in temperature in pile, α_{pile} = coefficient of linear thermal expansion of pile

Load transfer from the pile to the soil is expressed by load transfer coefficient: f_s for side resistance and f_b for bottom resistance.

$$dP = -f_s * z * dx * \pi * D$$

$$\frac{dP}{dx} = -f_s * z * \pi * D \quad (3)$$

where, f_s = side load transfer coefficient of soil, D = diameter of the pile, z = displacement of the pile segment, dx = length of the pile segment

Differentiating Equation 2 and equating with Equation 3:

$$EA\frac{d^2z}{dx^2} = f_s * z * \pi * D \quad (4)$$

Converting Equation 4 to the finite difference form:

$$\frac{EA(z_{i+1} + z_{i-1} - 2z_i)}{\Delta x^2} = f_s * z * \pi * D$$

On solving,

$$z_i = \frac{EA(z_{i+1} + z_{i-1})}{2EA + f_s \pi D \Delta x^2} \quad (5)$$

Boundary condition was applied in head and bottom of the pile.

At pile head:

$$P_{head} = -EA\frac{dz}{dx} + \Delta T \alpha_{pile} EA$$

$dz = z_1 - z_0$ so on solving

$$z_0 = z_1 - \Delta x\left(\Delta T\alpha_{pile} - \frac{P_{head}}{EA}\right) \quad (6)$$

where, P_{head} = load at top of the pile, z_0 = displacement of the pile top

At the tip (bottom of pile):

$$P_{tip} = z_{tip} * f_b$$

Also,

$$P_{tip} = -EA\frac{dz}{dx} + \Delta T\alpha_{pile}EA$$

Hence,

$$z_n = z_{n-1} + \Delta x\left(\Delta T\alpha_{pile} - \frac{P_{tip}}{EA}\right) \quad (7)$$

where, $z_n = z_{tip}$ = displacement of the pile at the bottom, f_b = bottom load transfer coefficient of soil, P_{tip} = reaction force developed in the pile bottom

Load displacement curve was obtained by implementing Equations 5, 6, and 7 in excel by iteration process. The axial strain in each segment was calculated based on the displacement of each segment.

$$\text{strain } (\epsilon) = \frac{\text{change of length of segment } (\Delta z)}{\text{original length } (\Delta x)}$$

Finally total axial force developed in each segment was calculated

$$P = \epsilon EA + \Delta T \alpha_{pile} EA$$

5.5 IMPLEMENTATION OF MODEL

Data obtained from the field test with thermal load of 5°C was used to estimate the soil parameters. Calibration of the model to match the field result obtained was done by checking various values of soil parameters in the model. Soil property values resulting in close approximation with field obtained data were finalized as soil properties for further use in analysis. Same soil properties were used to predict response at other thermal load and also in the parametric study. Finalized parameters of the model are summarized in Table 5-6.

Figure 5-10 shows axial strain measured in the field and the calculated strain at 5°C thermal load. Model data show close match with field obtained data.

Table 5-6: Parameter used in t-z model

Description	Value
Youngs Modulus of Pile (E_{pile})	25 Gpa
Load transfer coefficient for side (f_s)	7.5 MN/m^3 (upper layer)
	20 MN/m^3 (lower layer)
Load transfer coefficient for bottom soil (f_b)	100 MN/m^3
Thermal expansion coefficient of concrete (α_{pile})	12*10^{-6} /°C

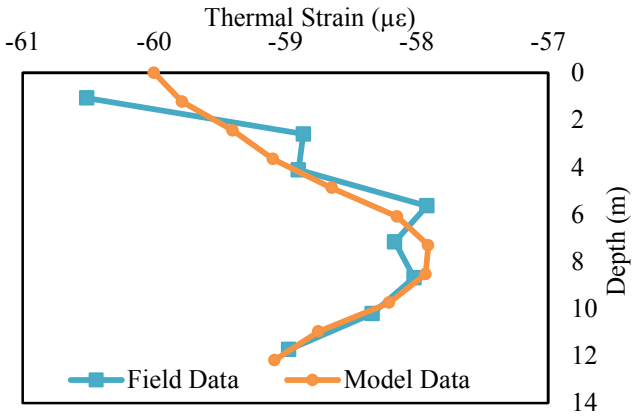

Figure 5-10: Field observed data and model calculated data at thermal load of 5°C

Validation of Estimated Parameter

Parameters calibrated by simulating thermal strain at 5°C thermal load were used to estimate the thermal strain induced at other thermal loads (7.5° C, 10° C, 15°C, 17.5° C, 19.3° C). Figure 5-11 shows the comparisons of field obtained data and modeled data.

Based on the results, the modified t-z model successfully predicted the thermal strain at different thermal load. The deviation between model and field data may be due to assumptions in the model. In the model, soil profile and soil properties were considered constant and uniform in all temperatures and along the length but in reality it varies. Also with change in temperature, soil may also expand or contract, which will result in different soil and pile interaction.

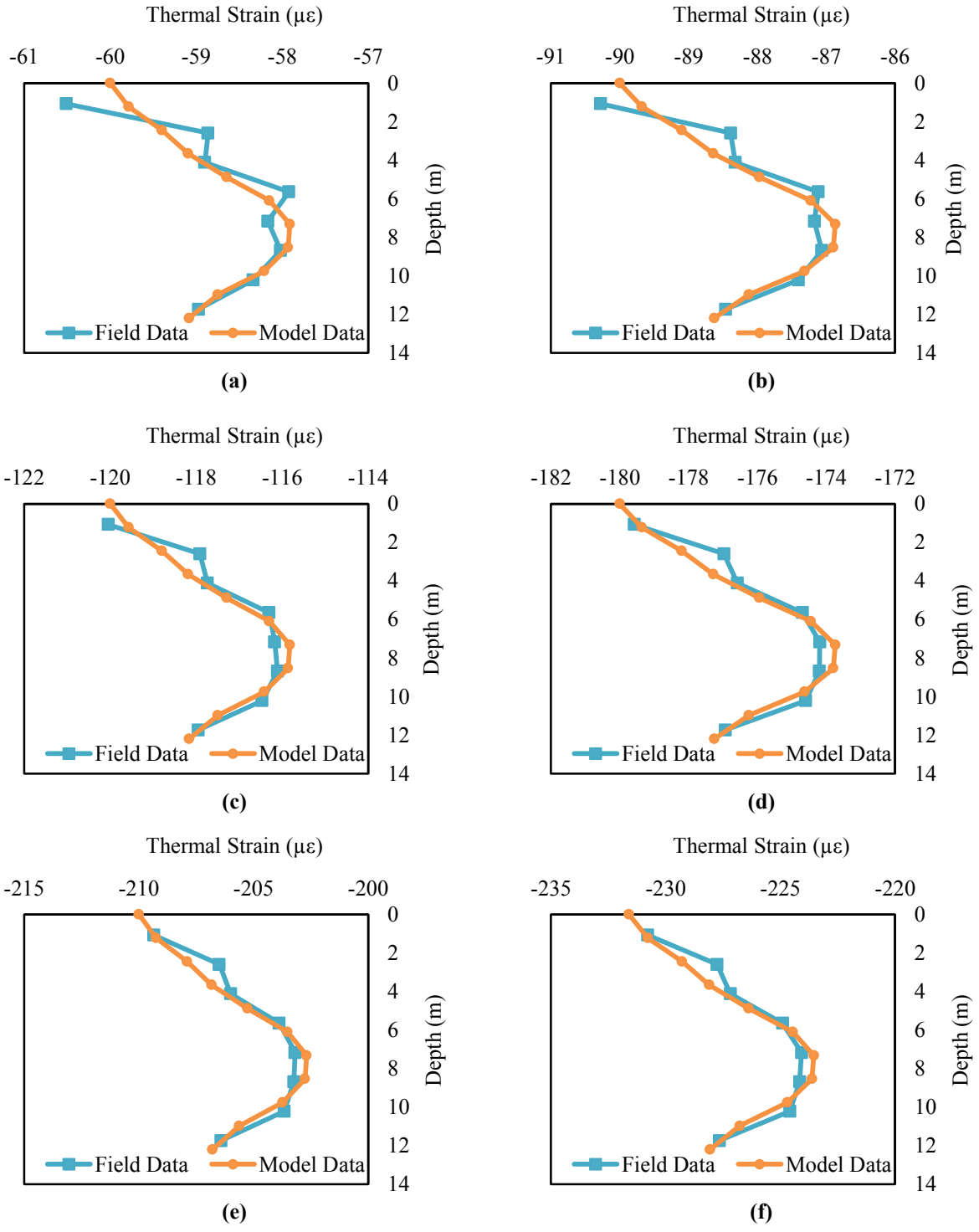

Figure 5-11: Comaparision of model estimated and observed strain at different thermal load: (a) 5° C, (b) 7.5° C, (c) 10° C, (d) 15° C, (e) 17.5° C, (f) 19.3°C

5.6 PARAMETRIC STUDY

The field test only gives pile response on particular field condition and a zero top load. In the parametric study, the effect of thermo-mechanical loading and soil load-transfer functions were investigated. Properties of base model considered for the parametric study are listed in Table 5-7.

Table 5-7: Base model properties

Description	Value
Temperature	10°C
Load	4 MN
Youngs Modulus of Pile (E_{pile})	25 Gpa
Load transfer coefficient for side (f_s)	7.5 MN/m^3 (upper layer) 20 MN/m^3 (lower layer)
Load transfer coefficient for bottom soil (f_b)	100 MN/m^3
Thermal expansion coefficient of concrete (α_{pile})	12*10^{-6} /°C

Thermo-mechanical loading

During the field test, the GHX-pile was only loaded with the heating thermal load. In this section, the t-z model developed was used to study the effect of combined application of mechanical and thermal load in the pile. Different vertical loads were applied at the pile head with different thermal loading (both heating and cooling). Response of the pile was observed in terms of force developed along the length of the pile and top displacement. Mechanical load of 3 MN, 4 MN and 5 MN were applied. Thermal load of -30° C, -20° C, -10° C, 0° C, 10° C, 20° C, and 30° C were applied.

Figure 5-12 shows the axial force along length of free head pile at various thermal loads. Compressive force developed along the length of the pile increases with the increase of

heating. With the increase of heating temperature, the pile tends to expand more and mobilized more side resistance causing an increase in compressive force. Result obtained from the model matched the result obtained in the field at similar thermal load (Figure 5-5). Under a cooling load, pile tends to contract, so a tension force was developed in the soil along the length of the pile. It causes less mobilization of side resistance. So, heating load increases mobilized force and cooling reduces it.

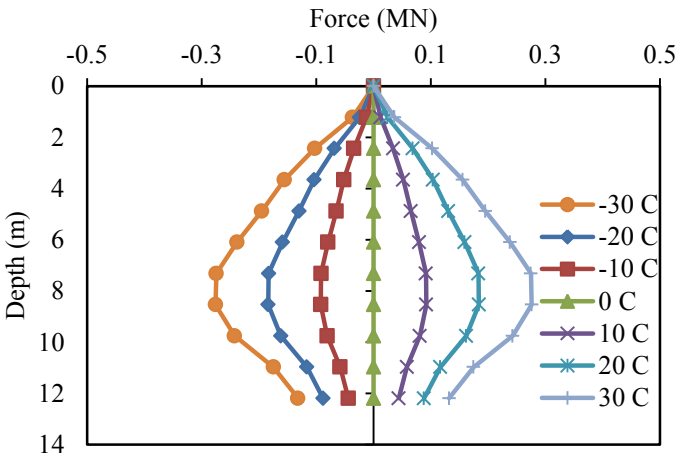

Figure 5-12: Variation of forces along the length of pile at different thermal load and free head condition

Figure 5-13 shows the variation of forces along the pile length on the application of thermo-mechanical loading. A mechanical load of 4 MN was applied with different thermal loads. As discussed earlier, heating increases mobilized axial force. Therefore, the pure mechanical loading curve (0°C thermal load) shifts to the right in the application of heating load. On cooling load shifts to the left. However, the variation in axial force due to the thermal load seems to be insignificant. Therefore, it can be assumed that there will be not much change in structural design of the pile due to additional normal thermal load, but that may not be the case for extreme thermal loading cases.

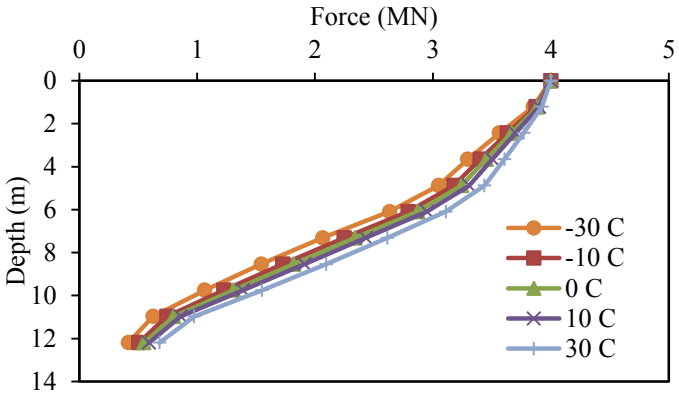

Figure 5-13: Variation of force with respect to depth in the pile at different temperatures and constant head load of 4 MN

Figure 5-14 shows top displacement of the pile with change in thermal loading at different head loads. The top displacement decreases on moving from the cooling load to the heating load because on heating pile tends to move up reduce downward displacement. Just reverse case was seen while moving towards cooling load from heating load. Predicted settlement might be more than a real case because there was no limitation applied in load transfer function in the model.

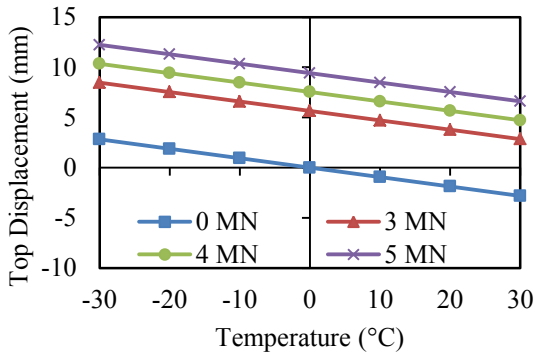

Figure 5-14: Variation of top displacement of the pile with change in thermal load at various constant head load.

Load Transfer Functions of Soil

The load transfer function depends on soil profile. The soil profile at the test site was divided in two layers. The profile consists of first 4 m of clay soil underlain by a rock layer. Estimation of these load transfer factors was done by simulation of the field result. Ranges of values of these parameters were tested in the model keeping other parameter constant to see the effect in the pile behavior. Effect of each case was compared in terms of variation of axial force along the length of the pile.

Figure 5-15 shows decrease of axial force developed with increase of side load transfer functions in both first (f_{s1}) and second layer (f_{s2}) of the soil. At same head load, with the increase of f_{s1} and f_{s2} soil becomes stronger and can bear more load causing less movement of the pile and less axial force.

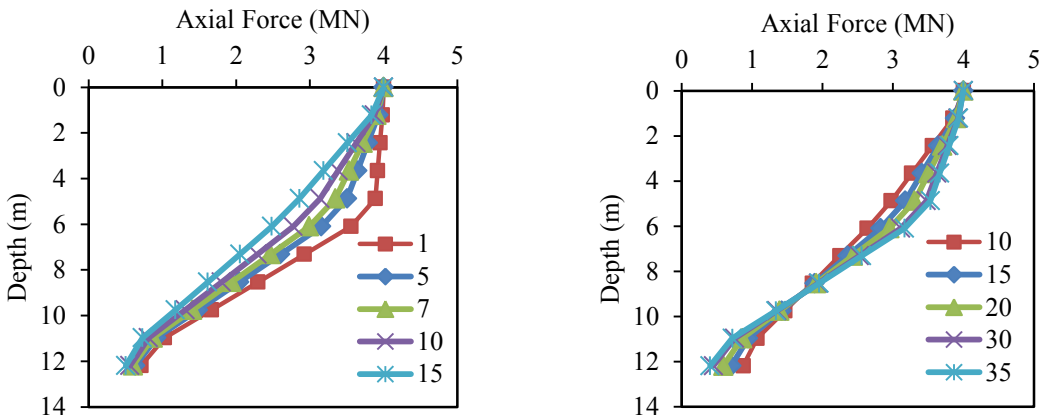

a. b.

Figure 5-15: Variation of axial force along the pile with different side load transfer functions on thermo-mechanical loading (Δ10° C, 4 MN) a) variation of top layer side load transfer function, b) variation of second layer side load transfer function

Same study was done for the tip load transfer function (f_b) and same response was obtained. With increase of f_b load bearing at bottom of the pile is more.

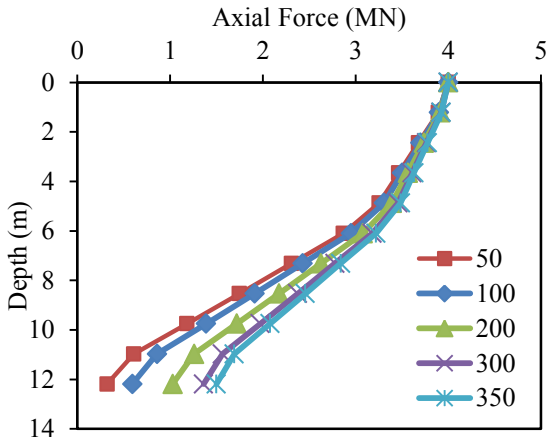

Figure 5-16: Variation of axial force along the pile with different bottom layer load transfer functions on thermo-mechanical loading (Δ10° C, 4 MN)

CHAPTER 6

CONCLUSIONS AND RECOMMENDATIONS

6.1 CONCLUSIONS

A geothermal heat exchanger pile of 1.067 m in diameter and 12.2 meter in depth was installed. The pile was equipped with eight U-loop heat exchanger pipes near the circumference. Eight vibrating wire strain gauges were installed at different depths along the centerline of the pile for measuring temperature and axial strain during the test. A thermal response test was conducted on the pile using a trailer device developed at OSU. Heat was supplied to the pile at the rate of 2000 W by circulating heat exchanger fluid in the pipes. A flow rate of 0.38 liter/sec was maintained in the pipes. The thermal response test was run for 39 days to achieve a significant rise in the pile and fluid temperature. A thermal load of 20°C was applied to the pile.

After completion of the test, thermal response test data were analyzed using the line source model. The applicability of this model on the large pile was studied by calculating the thermal conductivity of soil considering different span of data. Geotechnical behavior of the pile was studied by analyzing strain data obtained from the test.

A modified t-z model was developed to investigate the behavior of the pile. Field test data were successfully simulated by the modified t-z model. The following conclusions can be drawn from this study:

1 The range of ground thermal conductivity (1.60 to 1.65 Btu/hr*ft*F and 1.2 to 1.3 Btu/hr*ft*F) were obtained by using different length of data in the line source model. All values were in the typical range of shale thermal conductivity and shale was present in the major portion of the pile length. Therefore, analysis of thermal response test (run for a considerable longer period of time) data of large- diameter GHX-pile with this theory seems reasonable.

2 The research results indicated that the maximum thermal load (heating) that can occur in the similar large-diameter pile in similar soil and weather condition is 30°C.

3 The modified t-z model successfully simulated field result and can be used for thermo-mechanical analysis of the GHX-pile.

4 Heating load increases the mobilized axial force of the pile while cooling load decreases it. In the case of a loaded pile, the change in the mechanical response of GHX-pile due to additional thermal load is small. Heating load helps to reduce the top displacement, while cooling increases the top displacement.

6.2 RECOMMENDATIONS

Based on the experienced gain from the work lots of research area were came to focus. Due to the time limit and some technical difficulties these areas were not researched in the current study. Therefore, these research areas are presented here as future research topics and are outlined as follows:

1 Currently no work was found that compare performance of borehole and GHX-pile in terms of heat exchanging behavior in similar situations. Therefore, some studies are needed to develop ways to compare the feasibility and efficiency of these two systems.

2 Heat extraction or injection rate of the bigger pile should be studied with different number of loops and also best number of loops and configuration should be determined by conducting tests in various numbers of loops (2, 4, 6, and 8) and configuration (series, parallel).

3 Current t-z model was based on many assumptions and simplification. Therefore, following modification are recommended for future work in the model:

- Provision to determine load transfer function as per soil profile.
- Consideration of soil expansion or contraction (soil movement).
- Consideration of change of soil property during thermal loading.

4 Validation of the modified t-z model by conducting thermal-mechanical loading test of the GHX-pile.

REFERENCES

Abdelaziz, S., Olgun, C., and Martin, J. (2011). "Design and Operational Considerations of Geothermal Energy Piles." Geo-Frontiers 2011© ASCE 2011.

ASTM (2008). "Standard Test Method for Determination of Thermal Conductivity of Soil and Soft Rock by Thermal Needle Probe Procedure." D5334, West Conshohocken, PA.

ASTM (2010). "Standard Test Method for Steady-State Heat Flux Measurements and Thermal Transmission Properties by Means of the Guarded-Hot-Plate Apparatus." C177, West Conshohocken, PA.

ASTM (2012). "Standard Practice for Using a Guarded-Hot-Plate Apparatus or Thin-Heater Apparatus in the Single-Sided Mode." C1044, West Conshohocken, PA.

Austin, W. A. (1998). "Development of an in situ system for measuring ground thermal properties." Dissertation/Thesis.

Bose, J., Smith, M., and Spitler, J. "Advances in ground source heat pump systems-an international overview." Proc., 7th IEA Heat Pump Conference. 1: 313.

Bourne-Webb, P., Amatya, B., Soga, K., Amis, T., Davidson, C., and Payne, P. (2009). "Energy pile test at Lambeth College, London: geotechnical and thermodynamic aspects of pile response to heat cycles." Géotechnique, 59(3), 237-248.

Brandl, H. (2006). "Energy foundations and other thermo-active ground structures." Geotechnique, 56(2), 81-122.

Brettmann, T., and Amis, T. "Thermal Conductivity Evaluation of a Pile Group Using Geothermal Energy Piles." ASCE.

Carslaw, H. S., and Jaeger, J. C. (1959). "Conduction of heat in solids." Oxford: Clarendon Press, 1959, 2nd ed., 1.

Coyle, H. M., and Reese, L. C. (1966). "Load transfer for axially loaded piles in clay." Journal of Soil Mechanics & Foundations Div, 92(SM2, Proc Paper 4702).

Eskilson, P. (1987). Thermal analysis of heat extraction boreholes, Lund University.

Farouki, O. (1986). Thermal properties of soils, Trans Tech Publications, Clausthal-Zellerfeld, Germany.

Frank, R., and Zhao, S. R. (1982). “Estimation par les paramètres press-iométriques de l’enfoncement sous charge axiale de pieux forés dansdes sols fins.” Bull. Liaison Lab. Ponts Chaussees, 119, 17–24 (in French).

Fridleifsson, I. B., and Freeston, D. H. (1994). "Geothermal energy research and development." Geothermics, 23(2), 175-214.

Gao, J., Zhang, X., Liu, J., Li, K. S., and Yang, J. (2008). "Thermal performance and ground temperature of vertical pile-foundation heat exchangers: A case study." Applied Thermal Engineering, 28(17), 2295-2304.

Gehlin, S. (2002). "Thermal response test: method development and evaluation."

Hamada, Y., Saitoh, H., Nakamura, M., Kubota, H., and Ochifuji, K. (2007). "Field performance of an energy pile system for space heating." Energy and buildings, 39(5), 517-524.

Henderson, H., Carlson, S., and Walburger, A. "North American monitoring of a hotel with room size GSHPS." Proc., IEA 1998 room size heat pump conference,

Niagara Falls, Canada.

Hwang, S., Ooka, R., and Nam, Y. (2010). "Evaluation of estimation method of ground properties for the ground source heat pump system." Renewable energy, 35(9), 2123-2130.

Ingersoll, L., and Plass, H. (1948). "Theory of the ground pipe heat source for the heat pump." ASHVE transactions, 47(7), 339-348.

Ingersoll, L. R., Zabel, O. J., and Ingersoll, A. C. (1954). "Heat conduction with engineering, geological, and other applications."

Jung, K., Chun, B., Park, S., and Choi, H. (2013). "Test Construction of Cast-in-Place Concrete Energy Pile in Dredged and Reclaimed Ground." Journal of Performance of Constructed Facilities.

Kersten, M. S. (1949). Thermal properties of soils, University of Minnesota Institute of Technology Engineering Experiment Station.

Knellwolf, C., Peron, H., and Laloui, L. (2011). "Geotechnical analysis of heat exchanger piles." Journal of Geotechnical and Geoenvironmental Engineering, 137(10), 890-902.

Kusuda, T., and Achenbach, P. R. (1965). "Earth temperature and thermal diffusivity at selected stations in the United States." DTIC Document.

Laloui, L., Nuth, M., and Vulliet, L. (2006). "Experimental and numerical investigations of the behaviour of a heat exchanger pile." International Journal for Numerical and Analytical Methods in Geomechanics, 30(8), 763-781.

Lund, J. W., Freeston, D. H., and Boyd, T. L. (2011). "Direct utilization of geothermal

energy 2010 worldwide review." Geothermics, 40(3), 159-180.

Marshall, A. (1972). "The thermal properties of concrete." Building Science, 7(3), 167-74.

Mogensen, P. (1983). "Fluid to duct wall heat transfer in duct system heat storages." Document-Swedish Council for Building Research(16), 652-657.

Mustafa Omer, A. (2008). "Ground-source heat pumps systems and applications." Renewable and Sustainable Energy Reviews, 12(2), 344-371.

Ooka, R., Sekine, K., Mutsumi, Y., Yoshiro, S., and SuckHo, H. (2007). "Development of a ground source heat pump system with ground heat exchanger utilizing the cast-in place concrete pile foundations of a building." EcoStock.

Pahud, D., and Hubbuch, M. "Measured thermal performances of the energy pile system of the dock midfield at Zürich Airport." Proc., Proceedings European geothermal congress.

Péron, H., Knellwolf, C., and Laloui, L. "A method for the geotechnical design of heat exchanger piles." Proc., Geo-Frontiers 2011@ sAdvances in Geotechnical Engineering, ASCE, 470-479.

Quick, H., Meissner, S., Michael, J., and Arslan, U. "Innovative foundation systems for high-rise buildings." Proc., Proceedings of the 1st Intelligent Building Middle East Conference, 7th.

Rees, S. W., Adjali, M. H., Zhou, Z., Davies, M., and Thomas, H. R. (2000). "Ground heat transfer effects on the thermal performance of earth-contact structures." Renewable and Sustainable Energy Reviews, 4(3), 213-265.

Reese, L. C., Isenhower, W. M., and Wang, S.-T. (2006). Analysis and design of shallow

and deep foundations, Wiley Hoboken, NJ.

Salomone, L. A., Marlowe, J. I., Bose, J. E., Oklahoma State University. Division of Engineering, T., Consultants, S. T. S., and Electric Power Research, I. (1989). Soil and rock classification for the design of ground-coupled heat pump systems: field manual, Distributed by International Ground Source Heat Pump Association, Stillwater, Okla.

Seed, H. B., and Reese, L. C. (1957). "The action of soft clay along friction piles." American Society of Civil Engineers Transactions.

Singh, R. M., Bouazza, A., Wang, B., Barry-Macaulay, D., Haberfield, C., Baycan, S., and Carden, Y. (2011). "Geothermal Energy Pile: Thermal cum Static Load Testing."

Wood, C., Liu, H., and Riffat, S. (2010). "Comparison of a modelled and field tested piled ground heat exchanger system for a residential building and the simulated effect of assisted ground heat recharge." International Journal of Low-Carbon Technologies, 5(3), 137-143.

Yang, H., Cui, P., and Fang, Z. (2010). "Vertical-borehole ground-coupled heat pumps: a review of models and systems." Applied Energy, 87(1), 16-27.

VITA

ROMAN POUDYAL

Candidate for the Degree of

Master of Science

Thesis: THE THERMAL-MECHANICAL BEHAVIOR OF A MULTIPLE-LOOP GEOTHERMAL HEAT EXCHANGER PILE

Major Field: CIVIL ENGINEERING

Biographical:

Education:

Completed the requirements for the Master of Science in Civil Engineering at Oklahoma State University, Stillwater, Oklahoma in December, 2014.

Completed the requirements for the Bachelor of Science in Civil Engineering at Tribhuvan University, Kathmandu, Nepal in 2010.

Experience:

Worked as research assistant (Jan 2013 to Present) in Oklahoma State University, Stillwater, Oklahoma

Worked as Civil Engineer (Jan 2011 to Nov 2012) in Shah Consult International (P.) Ltd., Kathmandu, Nepal

Professional Memberships:

Student member: ASCE